

## **Supplementary Material and Methods**

### Experimental mice, adoptive transfer and infections

C57BL/6, *rag1<sup>-/-</sup>*, and congenic PTprc<sup>a</sup> mice were purchased from Australian Resource Center (Canning Vale) or bred in-house. PbTII, C57BL/6, *rag1<sup>-/-</sup>*, congenic PTprc<sup>a</sup> (CD45.1), nzEGFP, *IgalsI<sup>-/-</sup>* (Jackson Laboratory: Stock No: 006337), *LysM<sup>Cre</sup>* (Jackson Laboratory Stock No: 004781), ROSA26iDTR (*iDTR*) (Jackson Laboratory Stock No: 007900) mice, and all crosses were maintained under specific pathogen-free conditions within animal facilities at the Wellcome Trust Genome Campus Research Support Facility (Cambridge, UK), registered with the UK Home Office, or at QIMR Berghofer Medical Research Institute (Brisbane, Australia). All mice were female and used at 8-12 weeks of age. All animal procedures were in accordance with the Animals (Scientific Procedures) Act 1986 and approved by the Animal Welfare and Ethical Review Body of the Wellcome Trust Genome Campus, or in accordance with Australian National Health and Medical Research Council guidelines and approved by the QIMR Berghofer Medical Research Institute Animal Ethics Committee (approval no. A02-633M).

Spleens from PbTII donor mice were aseptically removed and homogenized through a 100µm strainer before erythrocytes lysis using RBC lysis buffer (eBioscience). CD4<sup>+</sup> T cells were enriched using CD4 microbeads (Miltenyi Biotech) and stained with CellTrace™ Violet (Invitrogen). Cells were injected (10<sup>6</sup>/200µl RPMI) via a lateral tail vein.

*PcAS* parasites were used after one *in vivo* passage in WT C57BL/6 mice. Mice were infected with 10<sup>5</sup> pRBCs i.v. and blood parasitemia was monitored by Giemsa-stained thin blood smears obtained from tail bleeds.

## Flow Cytometry

Single-cell suspensions were prepared by homogenizing spleens through 100 µm strainers and lysing erythrocytes using RBC lysis buffer (eBioscience). Prior to staining, Fc receptors were blocked using anti-CD16/32 antibody (BD Pharmingen or in-house). Intracellular staining was performed by first incubating cells in brefeldin-A (10 mg/ml) at 37°C for 3 hours. For IL-10/IFN $\gamma$  staining, cells were also incubated with Ionomycin (500 ng/ml) and PMA (25 ng/ml). Staining was performed using the eBioscience FoxP3 intracellular kit. For DNA/RNA staining, Hoechst33342 (10µg/ml; Sigma) was added at 1/500 v/v to cell preparation 15 minutes prior to acquisition using a BD LSРFortessa IV (BD Bioscience). Cells were sorted using a MoFlo XDP (Beckman Coulter), a FACSaria II (Becton Dickinson) or an Influx (Becton Dickinson) instrument. Activated PbTII cells were sorted as CD4 $^{+}$ TCR $\beta^{+}$  and CD69 $^{+}$  and/or divided at least once as measured using the CellTrace™ Violet proliferation dye. Dendritic cells were sorted as CD11c $^{\text{hi}}$ MHCII $^{\text{hi}}$ TCR $\beta^{-}$ B220 $^{-}$ . Naive dendritic cells were further sorted as CD8 $\alpha^{+}$ CD11b $^{-}$  or CD8 $\alpha^{-}$ CD11b $^{+}$ , and inflammatory monocytes as CD11b $^{\text{hi}}$ Ly6C $^{\text{hi}}$ Ly6G $^{\text{lo}}$ TCR $\beta^{-}$ B220 $^{-}$ .

## Single-cell capture and processing

Single cell processing with the Fluidigm C1 system was performed using small-sized capture chips (for 5-10µm cells). 1 µl of a 1:4000 dilution of External RNA Control Consortium (ERCC) spike-ins (Ambion, Life Technologies) was included in the lysis buffer. For processing with the Smart-seq2 protocol, the cells were sorted into 96-well plates containing lysis buffer. The lysis buffer consisted of Triton-X, RNase inhibitor, dNTPs, dT30 primer and ERCC spike-ins (Ambion, Life Technologies, final dilution 1:100 million). 24 cycles of cDNA amplification were performed. Libraries were prepared using Nextera XT DNA Sample Preparation Kit (Illumina), pooling up to

96 single cells. Pooled libraries were purified using AMPure XP beads (Beckman Coulter) and sequenced on an Illumina HiSeq 2500 instrument, using paired-end 100 or 125-base pair reads.

#### Processing and QC of scRNA-Seq data

Gene expression was quantified using Salmon, version 0.4.0. The parameter libType=IU, and a transcriptome index built on Ensembl version 78 mouse cDNA sequences. Sequences from the ERCC RNA spike-ins were included in the index, as well as 313 mouse-specific repeat sequences from RepBase. As quality control measures, we assessed the number of input read pairs, and the amount of mitochondrial gene content, considering cells with less than 100,000 reads or more than 35% mitochondrial gene content as failed. For T cells, we additionally considered cells where number of genes was less than  $100 + 0.008 * (\text{mitochondrial gene content})$  as failed. For the data generated using a 96-well plate-based Smart-seq2 protocol, which does not permit visual inspection of the captured cells, we additionally excluded low-quality cells from which fewer than 2000 genes were detected, motivated by negative control wells. To verify that the cells sorted in the wells were PbTII cells, we only selected cells from which both the transgenic TCR alpha and beta chains were detected (Supplementary Tables 2 and 3). For expression values, the Transcripts Per Millions (TPM's) estimated by Salmon included ERCC spike-ins. Thus, to obtain values representing only the *endogenous* RNAs, we removed ERCC's from the expression table and scaled the TPM's so they again summed to a million. We also globally removed genes from analysis where less than three cells expressed the gene at minimum 1 TPM, unless stated otherwise.

## Determining T cell receptor expression

T cell receptor sequences were reconstructed from scRNASeq data using the TraCeR software as previously described (47).

## Annotation of cell-surface receptors, cytokines and transcription factors

Genes likely to encode transcription factors, cell-surface receptors or cytokines were found by combining information from KEGG (<http://www.genome.jp/kegg/>), the Gene Ontology Consortium (<http://geneontology.org/>), PANTHER (<http://www.pantherdb.org/>) along with the more specific databases detailed below.

Transcription factors were found by searching the Gene Ontology Consortium database using the following ontology term: *GO:0003700 (sequence-specific DNA binding transcription factor activity)*; KEGG for *ko03000 (Transcription Factors)*; PANTHER for *PC00009 (DNA binding) AND PC00218 (Transcription Factors)*. The presence of genes in the following databases was also used as evidence for transcription factor activity: AnimalTFDB (<http://www.bioguo.org/AnimalTFDB/index.php>), DBD (<http://www.transcriptionfactor.org>), TFCat (<http://www.tfcat.ca>), TFClass (<http://tfclass.bioinf.med.uni-goettingen.de/tfclass>), UniProbe ([http://the\\_brain.bwh.harvard.edu/uniprobe](http://the_brain.bwh.harvard.edu/uniprobe)) and TFcheckpoint (<http://www.tfcheckpoint.org>).

Cell-surface receptors were found by searching the Gene Ontology Consortium database using the following ontology terms *GO:0004888 (transmembrane signaling receptor activity) OR GO:0008305 (integrin complex) AND NOT (GO:0004984 (olfactory receptor activity) OR GO:0008527 (taste receptor activity))*; KEGG for *ko04030 (G-Protein Coupled Receptors) OR*

*ko04050 (Cytokine Receptors) OR ko01020 (Enzyme-linked Receptors); PANTHER for PC00021 (G-Protein Coupled Receptors) OR PC00084 (Cytokine Receptors) OR PC00194 (Enzyme-linked Receptors).* Annotation of genes as receptors in the ImmPort (<https://immpport.niaid.nih.gov/>), GPCRDB (<http://gpcrdb.org/>) or IUPHAR (<http://www.guidetopharmacology.org/>) databases was also used as evidence for receptor functionality.

Cytokines were found by searching the Gene Ontology Consortium database using the following ontology terms *GO:0005125 (cytokine activity)*; KEGG for *ko04052 (Cytokines)*; PANTHER for *PC00083 (Cytokines)*. Annotation of genes as cytokines in ImmPort was also used in this case.

Genes were scored according to the number of databases and search results in which they occurred. Scores were weighted according to the strength of evidence provided by each database such that functional annotations supported by manually reviewed experimental evidence were given a higher score than those that were solely computationally generated (Table)

<u>Annotation source</u>	<u>Score</u>
<u>KEGG</u>	<u>3</u>
<u>Gene Ontology Consortium evidence codes IDA, IPI, IMP, IGI, IEP, ISS, ISO, ISA, ISM, IGC, IBA, IBD, IKR, IRD, RCA, TAS, IC</u>	<u>5</u>
<u>Gene Ontology Consortium evidence codes IEA, NAS, ND</u>	<u>1</u>
<u>PANTHER</u>	<u>2</u>

<u>AnimalTFDB</u>	<u>4</u>
<u>DBD</u>	<u>1</u>
<u>TFCat</u> , classed as ‘transcription factor’	<u>7</u>
<u>TFCat</u> , classed as ‘candidate’	<u>5</u>
<u>TFClass</u>	<u>4</u>
<u>UniProbe</u>	<u>7</u>
<u>TFcheckpoint</u> (if manually reviewed)	<u>6</u>
<u>ImmPort</u>	<u>4</u>
<u>GPRCDB</u>	<u>2</u>
<u>IUPHAR</u>	<u>7</u>

Genes were assigned as likely cell-surface receptors or cytokines if they had a cumulative score greater than or equal to 5 in that category. Genes were assigned as likely transcription factors if they had a cumulative score greater than or equal to 6 in that category.

#### In vivo cell depletion

Cellular depletion in *LysM*<sup>Cre</sup> x *iDTR* mice was performed by intraperitoneal injection of 10ng/g DT (Sigma-Aldrich) in 200μl 0.9% saline (Baxter) at day 3 post-infection. Control mice were

given 0.9% saline only. For B cell depletion, anti-CD20 (Genentech) or isotype control antibody was administered in a single 0.25mg dose via i.p. injection in 200ul 0.9% NaCl (Baxter), 7 days prior to infection.

### Confocal microscopy

Confocal microscopy was performed on 10–20  $\mu\text{m}$  frozen spleen sections. Briefly, splenic tissues were snap frozen in embedding optimal cutting temperature (OCT) medium (Sakura) and stored at -80°C until use. Sections were fixed in ice-cold acetone for 10 minutes prior to labeling with antibodies. DAPI was used to aid visualization of white pulp areas. Samples were imaged on a Zeiss 780-NLO laser-scanning confocal microscope (Carl Zeiss Microimaging) and data analyzed using Imaris image analysis software, version 8.1.2 (Bitplane). Cells were identified using the spots function in Imaris, with thresholds <10mM and intensities <150. All objects were manually inspected for accuracy before data were plotted and analyzed in GraphPad prism (version 6).

## **Supplementary figure and table captions**

**Table S1** The expression data from day 7 p.i. with functional annotations for genes (external file).

Th1 annotations are based on studies by Hale *et al.* (SMARTA transgenic, day 6 of LCMV infection, CXCR5<sup>-</sup>Ly6c<sup>hi</sup>), Marshall *et al.* (SMARTA transgenic, day 8 of LCMV infection, PSGL1<sup>hi</sup>Ly6c<sup>hi</sup>), Stubbington *et al.* (*In vitro*, day 4)(15, 44, 45). Tfh annotations are based by studies by Hale *et al.* (CXCR5<sup>+</sup>Ly6c<sup>lo</sup>, Marshall *et al.* (PSGL1<sup>lo</sup>Ly6c<sup>lo</sup>) and Liu *et al.* (Bcl6-RFP reporter, KLH immunization, CXCR5<sup>+</sup>Bcl6<sup>hi</sup>) (37). Th2 and Th17 annotations are based on Stubbington *et al.* and annotations for genes associated with exhausted CD4<sup>+</sup> T cell phenotype are based on Crawford *et al.* (Day 30 of LCMV infection, genes upregulated in exhausted cells but not in memory cells)(49).

**Table S2** TraCeR detection statistics for T cell receptor sequences in single-cell RNA-seq data from the first set of experiments, performed using the C1 platform (external file).

**Table S3** TraCeR detection statistics for T cell receptor sequences in single-cell RNA-seq data from the second set of experiments, performed using the Smart-seq2 platform (external file).

**Table S4** Annotation of receptors, cytokines and transcription factors (external file). The annotation strategy is described in Supplementary material and methods.

## Figure S1

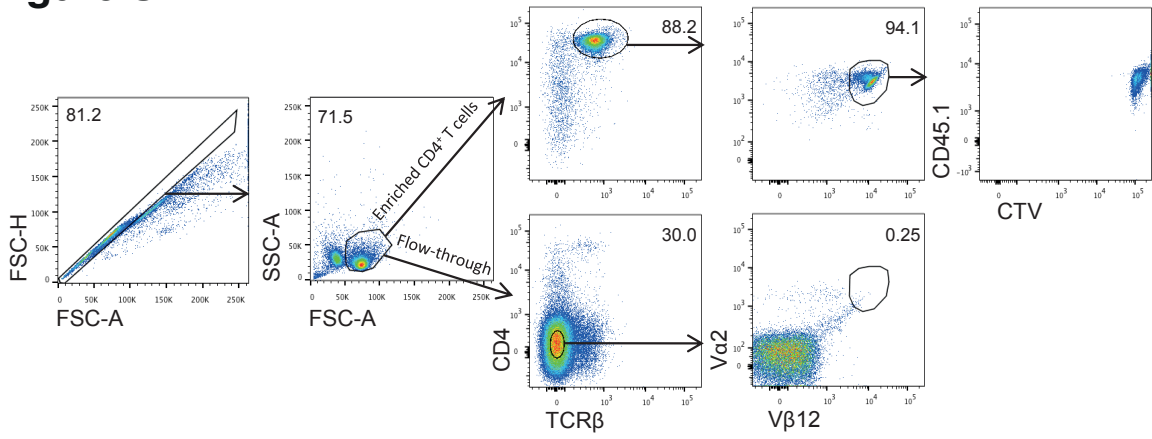


**Fig. S1.** Enrichment of PbTII cells for adoptive transfer.

**(A)**  $\text{CD4}^+$  T cells were enriched using positive selection (MACS microbeads) from the spleen of a naive, PbTII x CD45.1 mouse. FACS plots show purity, expression of V $\alpha$ 2 and V $\beta$ 12 transgenes, and CellTrace™ Violet (CTV) staining of enriched PbTII cells compared to corresponding flow-through from the enrichment process.

**Figure S2**

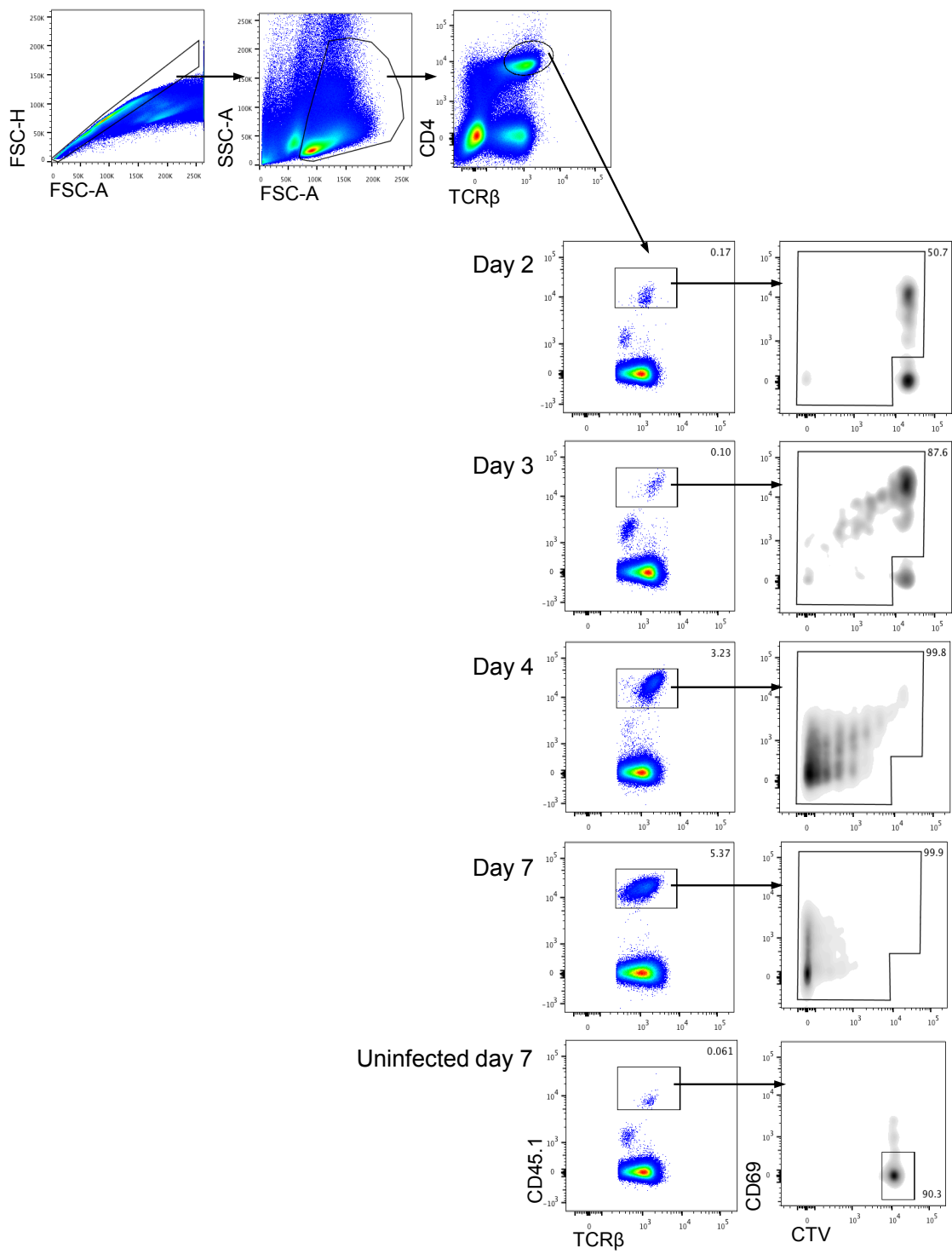


**Fig. S2.** Sorting strategy for PbTII cells.

(A) PbTII cells ( $CD4^+ TCR\beta^+ CD45.1^+$ ) were adoptively transferred into WT congenic ( $CD45.2^+$ ) recipient mice. At indicated days, early activated ( $CD69^+$ ) and/or proliferated ( $CTV^{lo}$ ) PbTII cells were cell-sorted from spleens of *PcAS*-infected mice, and naïve PbTII cells ( $CD69^{lo} CTV^{hi}$ ) were cell-sorted from the spleens of naïve mice at day 7 post-transfer.

## Figure S3

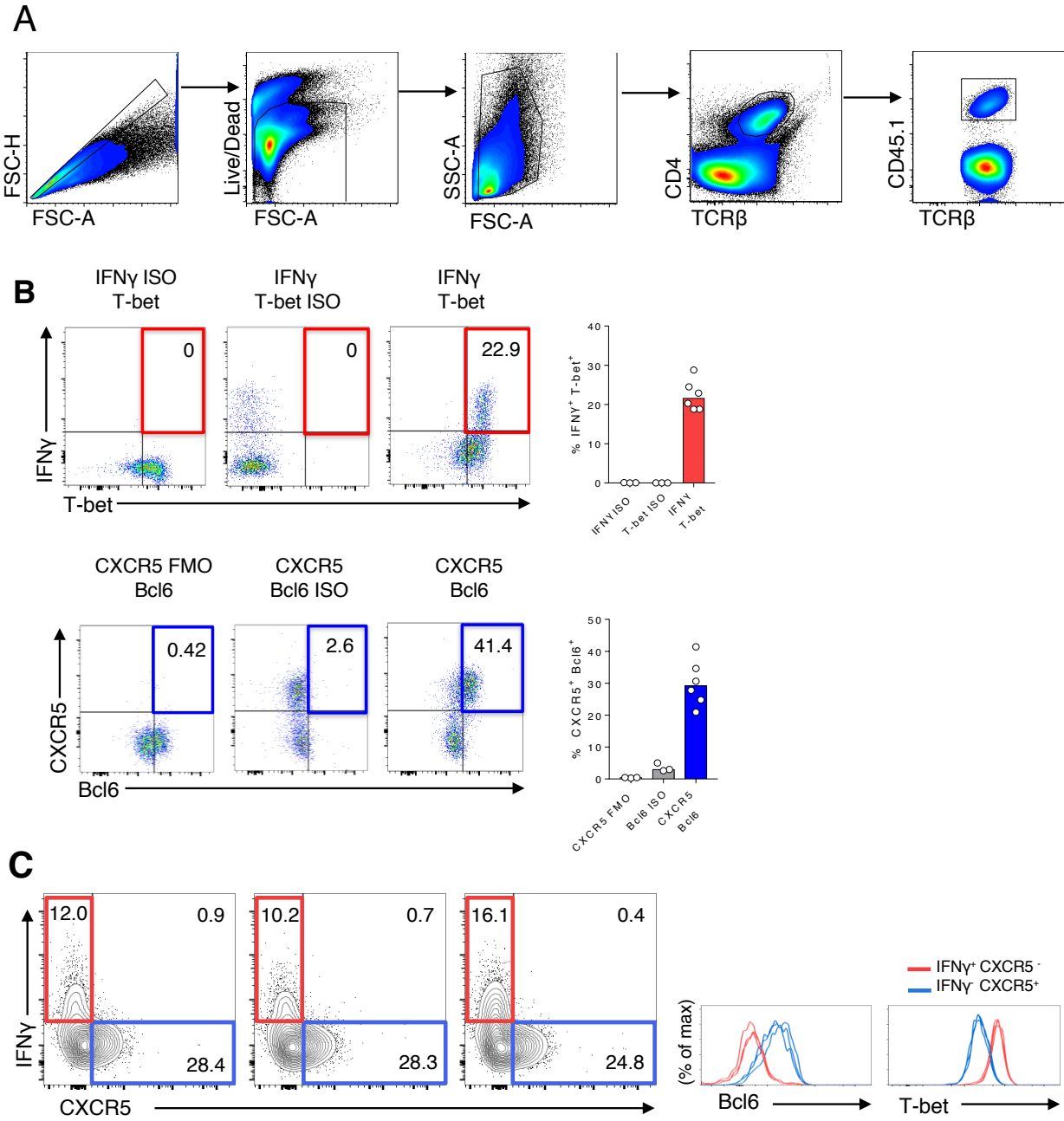


**Fig. S3.** Flow cytometric assessment of Th1/Tfh responses during *PcAS* infection.

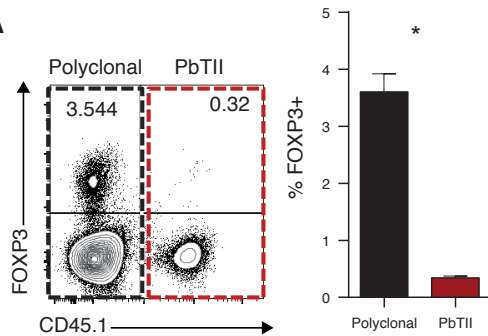
**(A)** Flow cytometric gating strategy employed to analyze splenic PbTII responses throughout this manuscript.

**(B)** Isotype controls for direct *ex vivo* intracellular staining of IFN $\gamma$ , T-bet and Bcl6, and fluorescence minus one (FMO) control for staining of CXCR5 expression by splenic PbTII cells from day 7-infected mice.

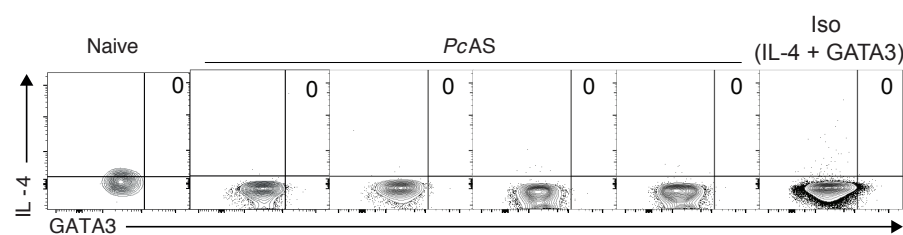
**(C)** Remaining FACS plots from data in Fig. 1B-C, showing expression of T-bet and Bcl6 by IFN $\gamma^+$  or CXCR5 $^+$  splenic PbTII cells at day 7 post-infection with *PcAS*. Each plot represents an individual mouse.

**Figure S4**

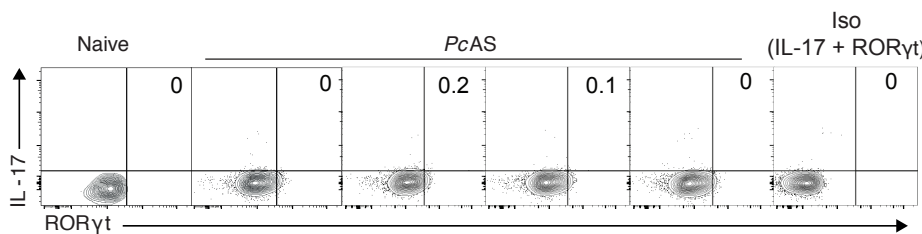
**A**



**B**



**C**



**D**

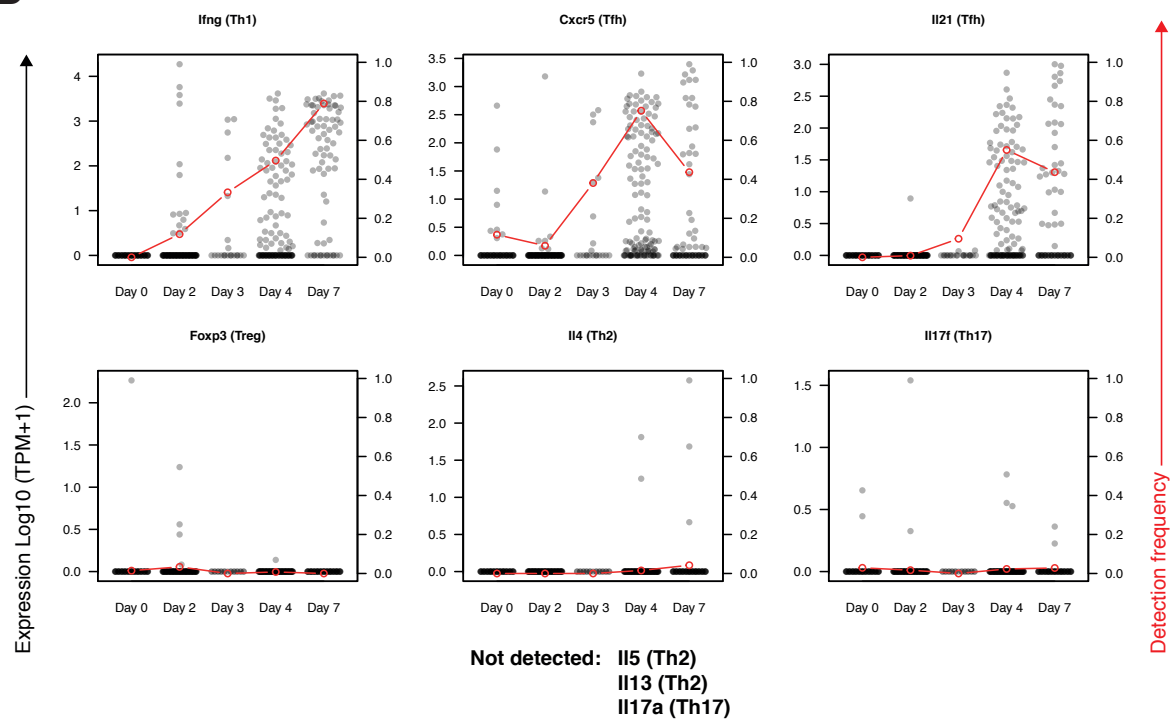


**Fig. S4.** Expression of subset-specific marker genes in PbTII cells.

- (A)** Representative FACS plot (gated on CD4<sup>+</sup> TCRβ<sup>+</sup> live singlets) and proportion of FOXP3<sup>+</sup> (Treg) splenic PbTII ( $10^4$  transferred) (CD45.1<sup>+</sup>; red dashed box) or polyclonal CD4<sup>+</sup> T (CD45.1<sup>-</sup>; black dashed box) cells from mice (n=6) at day 7 post-infection.
- (B-C)** FACS plots (gated on CD45.1<sup>+</sup> CD4<sup>+</sup> TCRβ<sup>+</sup> live singlets) of (B) IL-4<sup>+</sup>GATA3<sup>+</sup> (Th2) and (C) IL-17<sup>+</sup>RORγt<sup>+</sup> (Th17) splenic PbTII cells in naive (receiving  $10^6$  cells) or *PcAS*-infected mice (receiving  $10^4$  cells) at day 7 post-infection. (A-C) Data are representative of two independent experiments. Statistics: Mann-Whitney U test; \*p<0.05.
- (D)** The mRNA expression of selected subset-specific cytokines and the Treg hallmark transcription factor *Foxp3* in PbTII cells. The red dots and line indicate the fraction of cells in each time point where the particular mRNA was detected.

## Figure S5

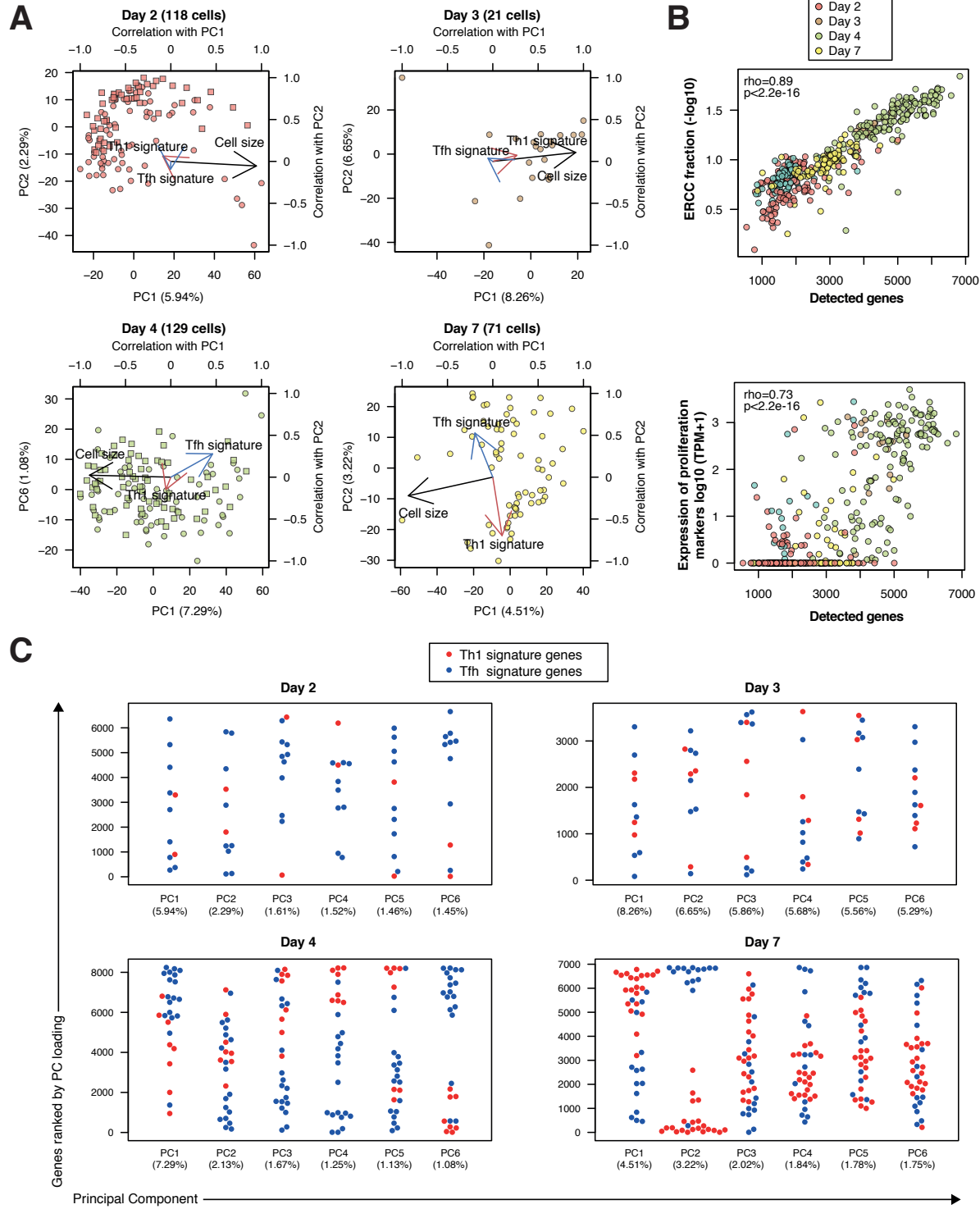


**Fig. S5.** Heterogeneity of activated PbTII cells and variability associated with cell size and differentiation.

**(A)** PCA of single PbTII cells at 2, 3, 4 and 7 days post-infection with *PcAS*. The PCA was based on all genes expressed at  $\geq 100$  TPM in at least 2 cells. The arrows represent the Pearson correlation with PC1 and PC2. Cell size refers to the number of detected genes. “Th1 signature” and “Tfh signature” refer to cumulative expression of top 30 signature genes associated with Th1 and Tfh phenotypes (15). The numbers in parenthesis show proportional contribution of respective PC.

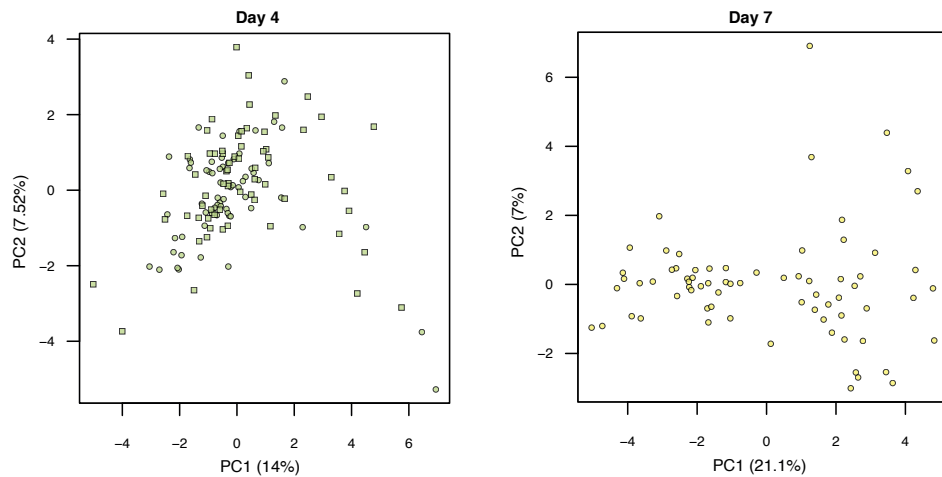
**(B)** The relationship of detected cell number with the fraction or reads mapping to ERCC spike-in RNA (top) and with cumulative expression of proliferation markers *Mki67*, *Mybl2*, *Bub1*, *Plk1*, *Ccne1*, *Ccndl1* and *Ccnb1* (31) (Figure 4B and S9).

**(C)** Ranked loading scores for PC1-PC6 of the Th1 and Tfh signature genes in the PCA shown in (A). The numbers in parenthesis show proportional contribution of respective PC.

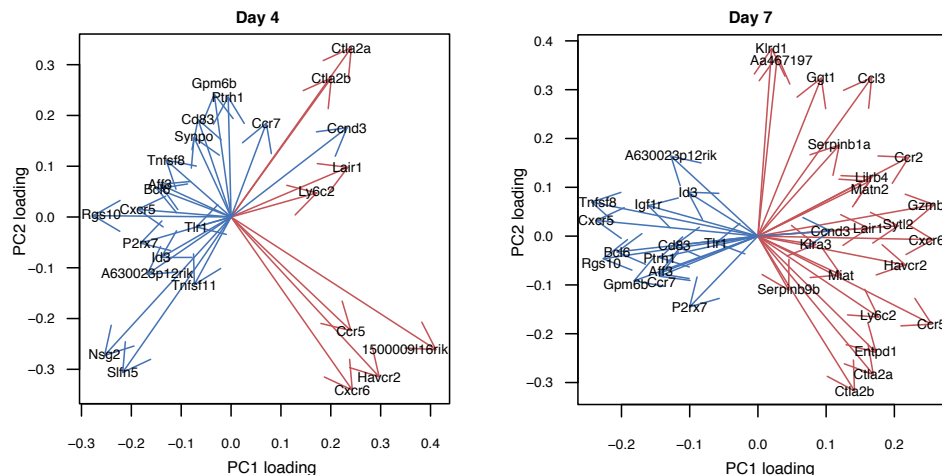
## Figure S6

**A**

Principal component analysis: Th1/Tfh signature genes



**B**



**C**

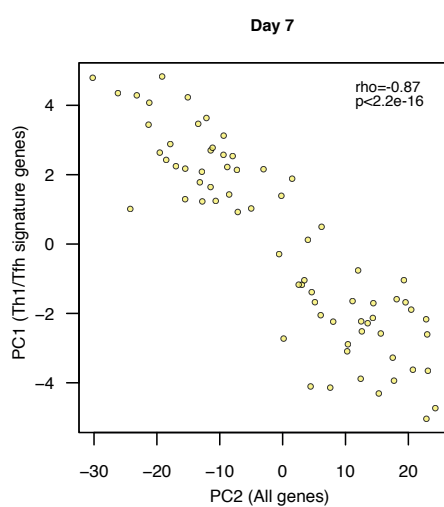


**Fig. S6.** Heterogeneity of Th1/Tfh signature gene expression in activated PbTII cells.

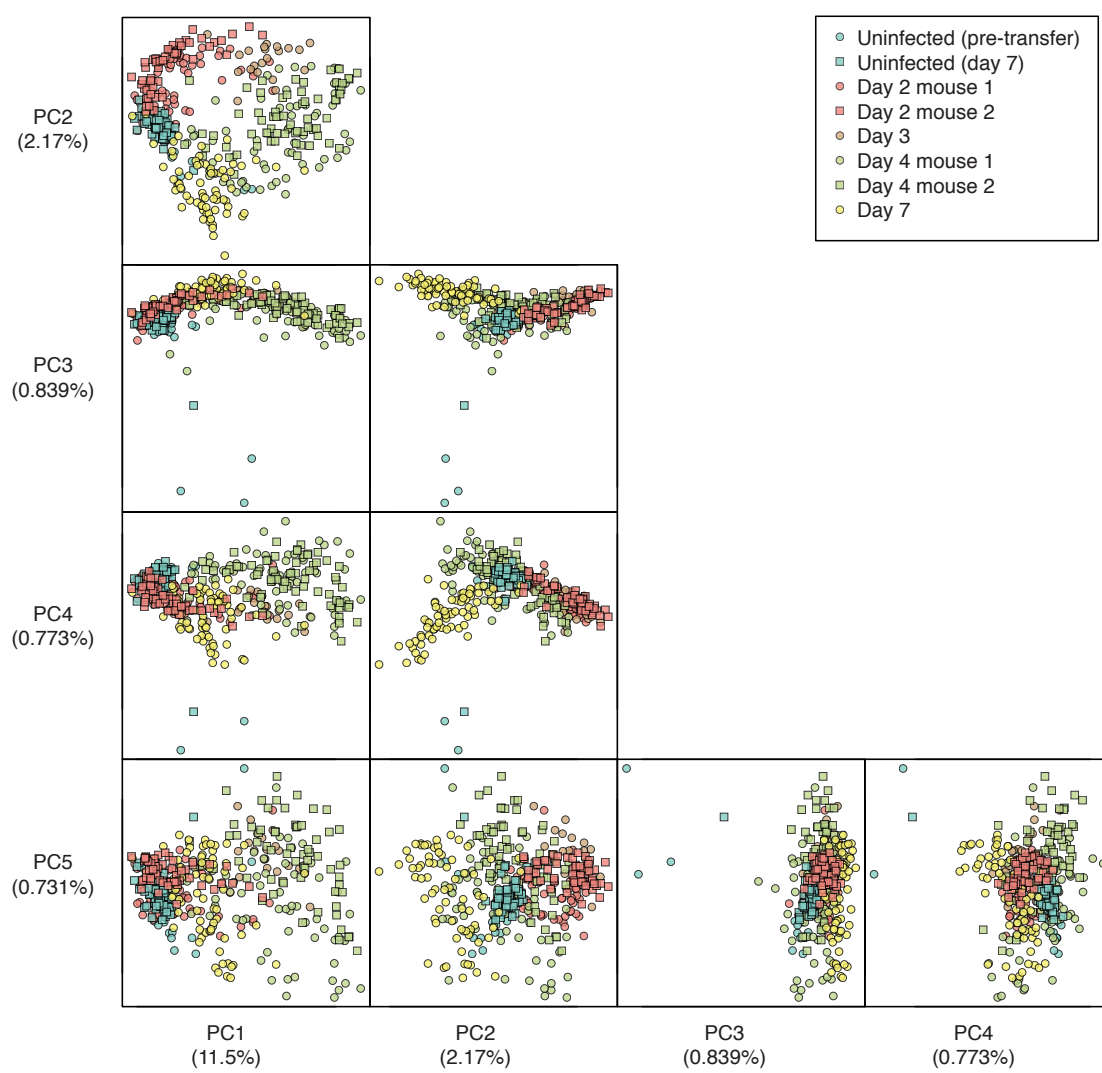
(A) Principal component analyses of day 4 (left) and day 7 (right) PbTII cells were performed using established Th1/Tfh signature genes (15) detected at the level  $\geq 100$  TPM in at least 2 cells. The numbers in parenthesis show proportional contribution of respective PC.

(B) The PC1 and PC2 loadings of individual Th1 (red) and Tfh (blue) signature genes in PCA of day 4 and day 7 PbTII cells (A).

(C) The correlation of PC1 from the analysis with the signature genes alone and PC2 of the genome-wide analysis (Figure 1E).

**Figure S7**

**A**



**B**

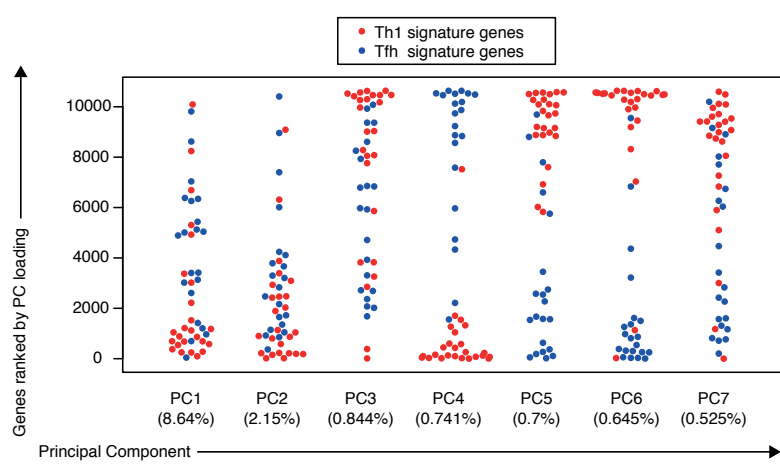


**Fig. S7.** Heterogeneity of the entire PbTII time series and the contribution of Th1 and Tfh signature genes to the overall variability.

**(A)** The first five components of the Principal Component Analysis of the entire time series. The numbers in parenthesis show proportional contribution of respective PC.

**(B)** The rankings of the Th1 and Tfh signature genes among the loadings of Principal Components 1-7.

**Figure S8**

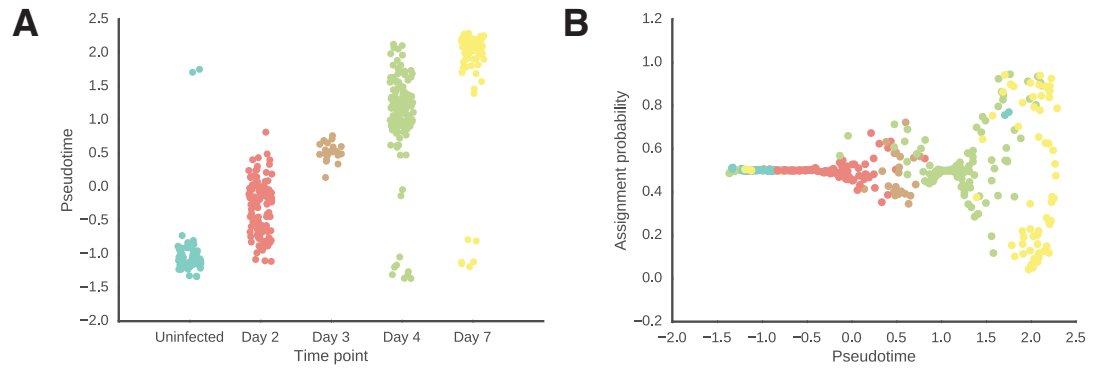
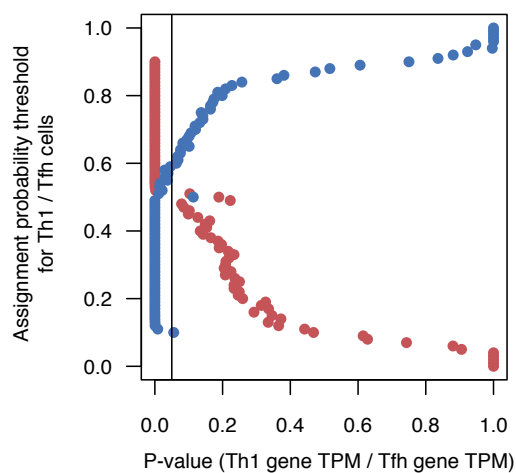


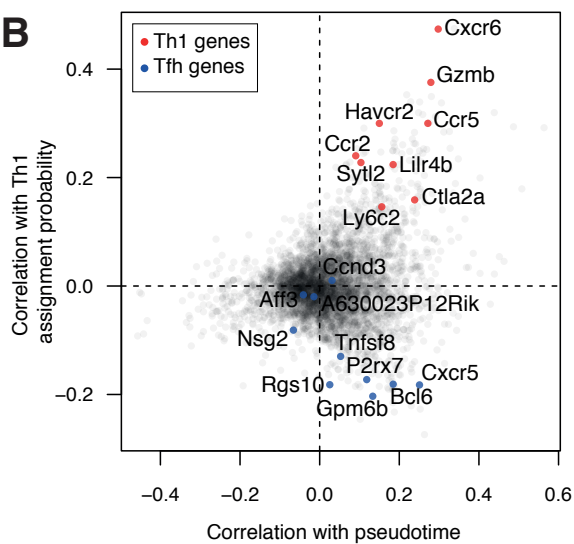
**Fig. S8.** The relationship of pseudotime with time points (**A**) and with the Th1 assignment probability (**B**).

**Figure S9**

**A**



**B**



**C**

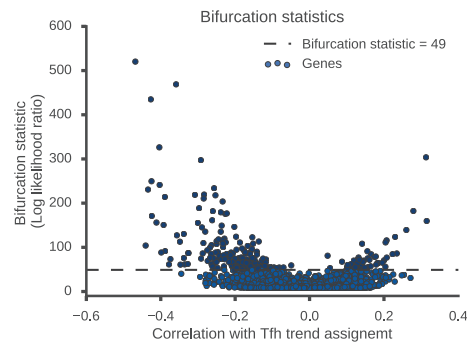


**Fig. S9.** Correlation of GPfates trends with Th1 and Tfh signature genes.

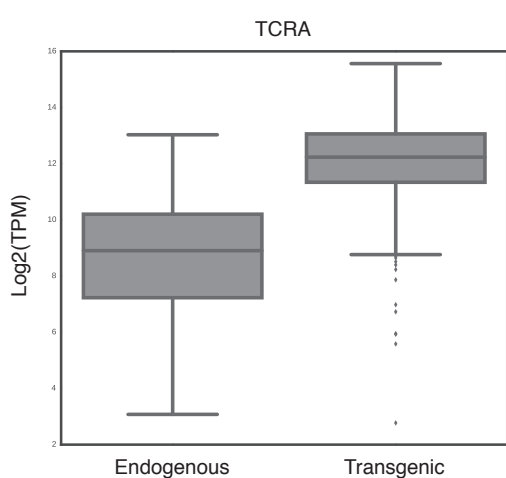
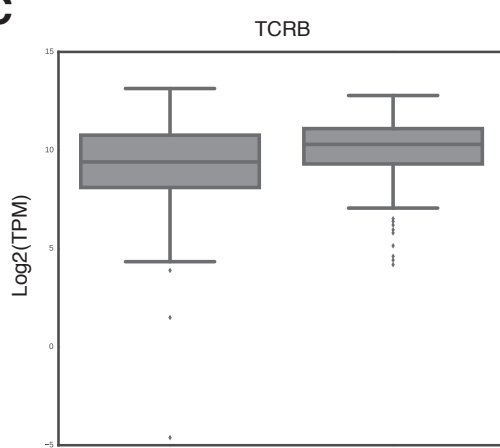
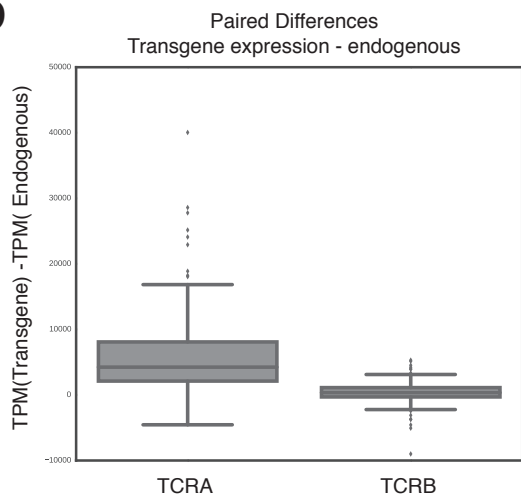
**(A)** The effect of the probability threshold on the cumulative expression of Th1 and Tfh signature genes (15). The p-values were calculated using Wilcoxon rank sum test.

**(B)** Correlation of expression of Th1 and Tfh signature genes with pseudotime and with Th1 assignment probability.

**(C)** Relation between genes expression correlation with mixture assignment probability, and the *bifurcation statistic*, for each gene. The threshold of bifurcation statistic = 49 has some stronger effect sizes. This is analogous to a *volcano plot* in classical differential expression testing.

**Figure S10****A**

		TCRB		
		Transgenic	Endogenous	Not detected
TCRA	Transgenic	287	15	76
	Endogenous	0	2	1
	Not detected	4	5	18

**B****C****D**

**Fig. S10.** Expression of transgenic and endogenous TCRs.

- (A) Statistics of TCR sequence detection. Numbers correspond to single cells in which the corresponding transcript was detected.
- (B) Expression levels ( $\log_2(\text{TPM})$ ) of for the endogenous or transgenic TCR $\alpha$  chains across the entire dataset.

**Figure S11**

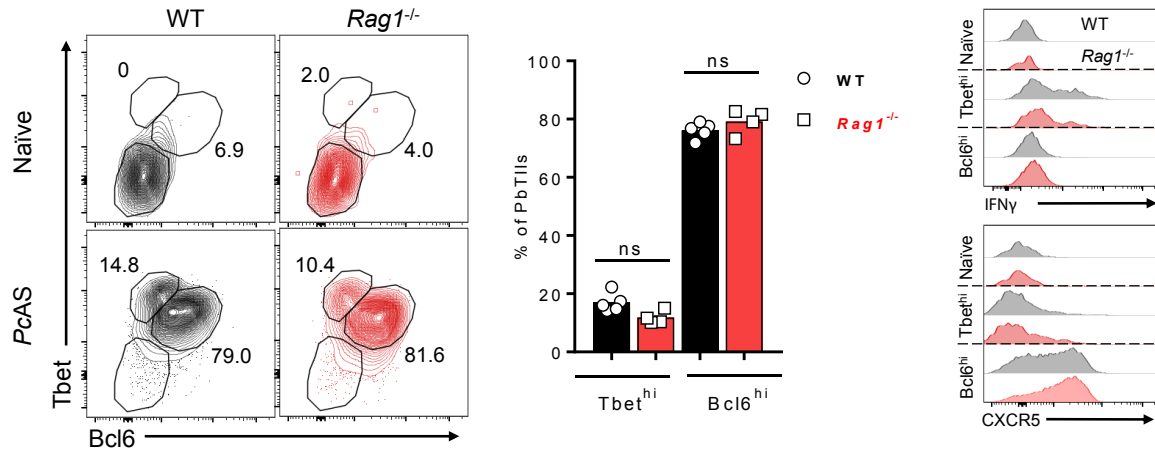


**Fig. S11.** Expression of endogenous TCRs does not influence PbTII cell Th1/Tfh differentiation.

(A) Representative FACS plots (gated on CD45.1<sup>+</sup> (WT) or CD45.2<sup>+</sup> (*Rag1*<sup>-/-</sup>), CD4<sup>+</sup> TCR $\beta^+$  V $\beta$ 12<sup>+</sup> live singlets) showing expression of T-bet or Bcl6 by splenic WT or *Rag1*<sup>-/-</sup> PbTII cells ( $10^4$  transferred into congenic recipient mice) at day 7 p.i. with *PcAS* (n=4).

(B) Summary graphs of proportions of WT or *Rag1*<sup>-/-</sup> PbTII cells exhibiting T-bet<sup>hi</sup> and Bcl6<sup>hi</sup> phenotypes from (A).

(C) Representative histograms of CXCR5 and IFN $\gamma$  expression by T-bet<sup>hi</sup> or Bcl6<sup>hi</sup> WT and *Rag1*<sup>-/-</sup> PbTII cells from (A) & (B). Statistics: Mann-Whitney U test; NS, not significant.

**Figure S12**

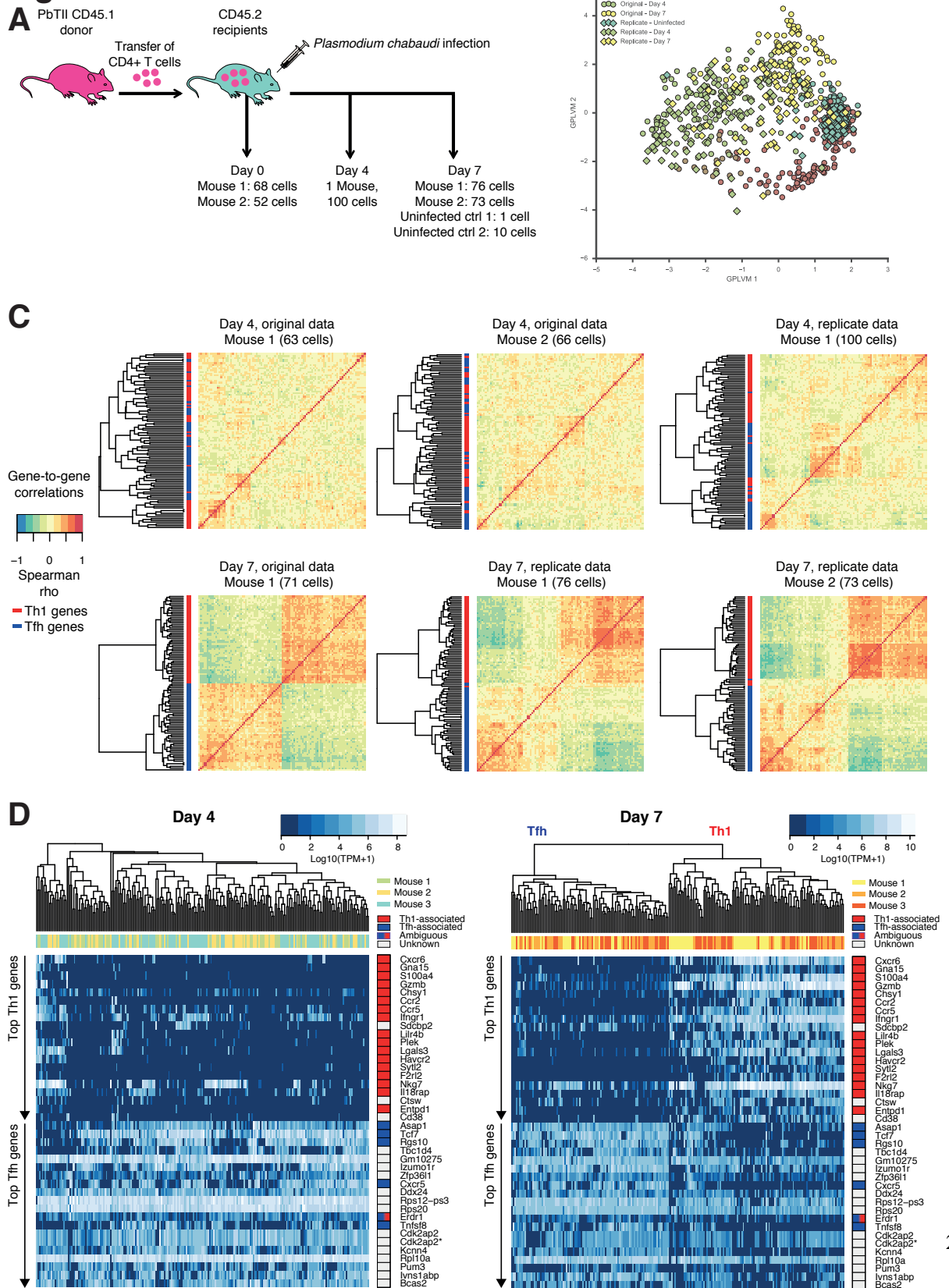
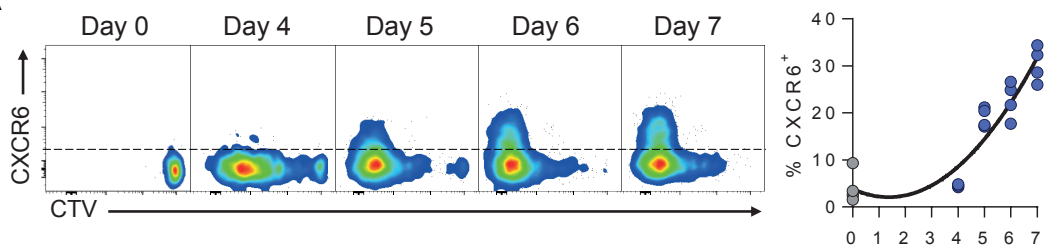


**Fig. S12.** Robustness of top bifurcating genes across experiments.

- (A)** Experimental design for the replicate *PcAS* infection. Single cells were sorted into 96-well plates and cDNA was amplified using the Smart-seq2 protocol.
- (B)** Bayesian Gaussian Process Latent Variable model of the combination of original and replicate data. The BGPLVM was fitted using the residuals from an ordinary least squares model of expression from the categorical variable of experiment, equivalent to `limma::removeBatchEffect`. Replicate data groups with corresponding data from the original experiment, illustrating that both experiments capture the same transcriptional landscape.
- (C)** The emergence of subset-specific gene patterns at day 7 of infection. For the top bifurcating genes (Fig S5C) pairwise gene-to-gene Spearman correlations were calculated. The rowside colours represent the association of the gene with either Th1 fate (red) or Tfh fate (blue).
- (D)** The expression of top 20 Th1 and Tfh associated genes identified using GPfates in single PbTII cells at days 4 and 7. The genes were annotated as Th1- or Tfh-associated based on public datasets (15, 37, 44, 45). \**Cdk2ap2* appears twice because two alternative genomic annotations exist.

**Figure S13**

**A**



**B**

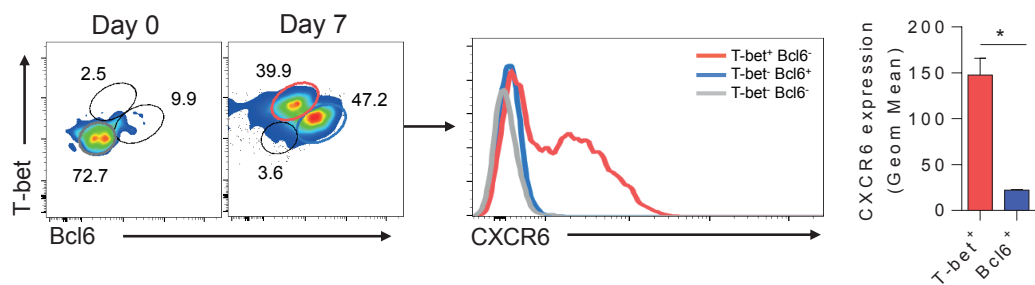


**Fig. S13.** Flow cytometric validation of CXCR6 expression in PbTII cells prior to and after bifurcation.

**(A)** Representative FACS plots showing kinetics of CellTrace<sup>TM</sup> Violet (CTV) dilution and CXCR6 expression, with summary graphs showing proportion of PbTII cells expressing this (after  $10^6$  PbTII cells transferred) in un-infected (Day 0) and *PcAS*-infected mice at indicated days post-infection (n=4 mice/time point, with individual mouse data shown in summary graphs; solid line in summary graphs indicates results from third order polynominal regression analysis.) Data are representative of two independent experiments. **(B)** Representative FACS plots showing CXCR6 expression in Tbet<sup>hi</sup> (red gate) and Bcl6<sup>hi</sup> (blue gate) PbTII cells, compared to naïve PbTIIIs (gray) at 7 days post-infection. Summary graph shows mean & standard deviations for geometric mean fluorescence intensity of CXCR6 expression in gated PbTII populations (n=4 mice) Statistics: Mann-Whitney U test \*p<0.05.

**Figure S14**

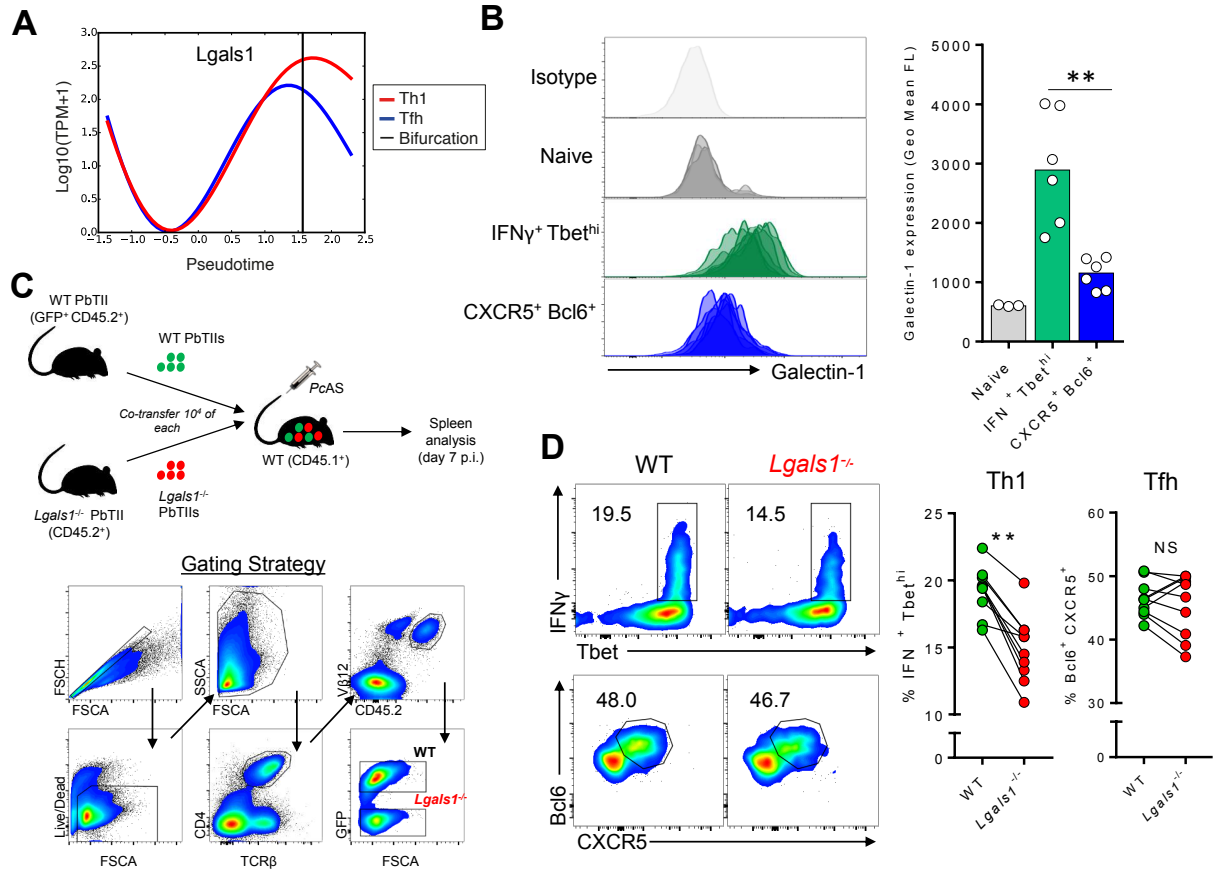


**Fig. S14.** T cell-intrinsic Galectin-1 supports Th1 fate commitment.

**(A)** Expression of *Lgals1* in the GPfates model across pseudotime. Curves represent Th1 (red) and Tfh (blue) trends when weighing the information from data points according to trend assignment.

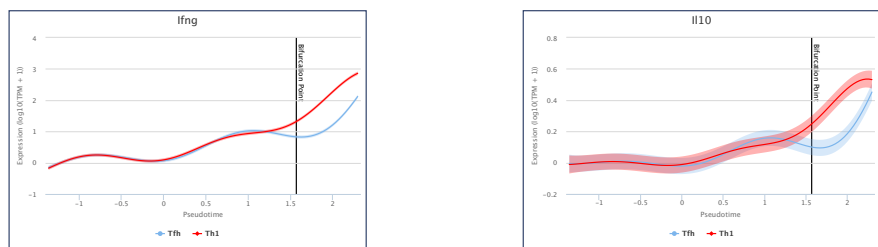
**(B)** Histograms of Galectin-1 expression by splenic PbTII cells ( $n=3-6$  mice per group, all data shown overlaid within each groups) and proportions expressing Galectin-1 in naïve mice ( $10^6$  transferred; gray), and by Th1 (T-bet<sup>hi</sup>  $\text{IFN}\gamma^+$ ; blue) and Tfh (Bcl6<sup>hi</sup> CXCR5<sup>+</sup>; green) cells ( $10^4$  transferred) in *PcAS*-infected mice at day 7 post-infection. Statistics: Mann-Whitney U Test; \*\*  $p<0.01$ . Data are representative of two independent experiments.

**(C)** Schematic showing co-transfer of WT ( $\text{GFP}^+$   $\text{CD45.2}^+$ ) and  $Lgals1^{-/-}$  ( $\text{CD45.2}^+$ ) PbTII cells ( $10^4$  of each transferred) into WT congenic  $\text{CD45.1}^+$  recipient mice (n=10), and gating strategy for assessment of splenic PbTII cells at 7 days post-infection.

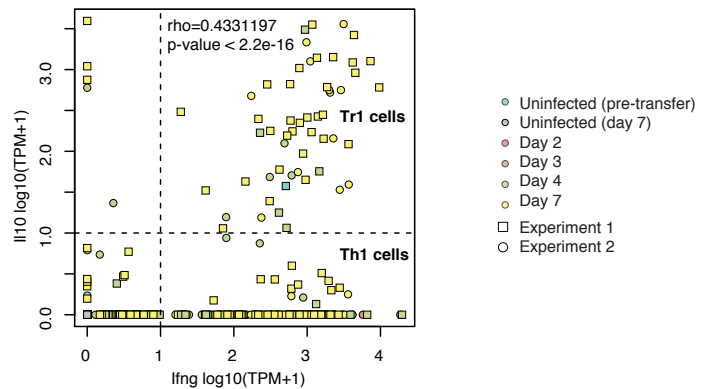
**(D)** Representative FACS plots (gated on  $\text{GFP}^+$  or  $\text{GFP}^-$ ,  $\text{CD45.2}^+$   $\text{CD4}^+$   $\text{TCR}\beta^+$   $\text{V}\beta12^+$  live singlets) and paired analysis of proportions of splenic WT and  $Lgals1^{-/-}$  PbTII cells exhibiting T-bet<sup>hi</sup>  $\text{IFN}\gamma^+$  (Th1) and  $\text{Bcl6}^{\text{hi}}$   $\text{CXCR5}^+$  (Tfh) phenotypes in mice described in (C). Statistics: Wilcoxon signed-rank Pairwise T-test; \*\*p<0.01; NS, not significant.

# Figure S15

**A**

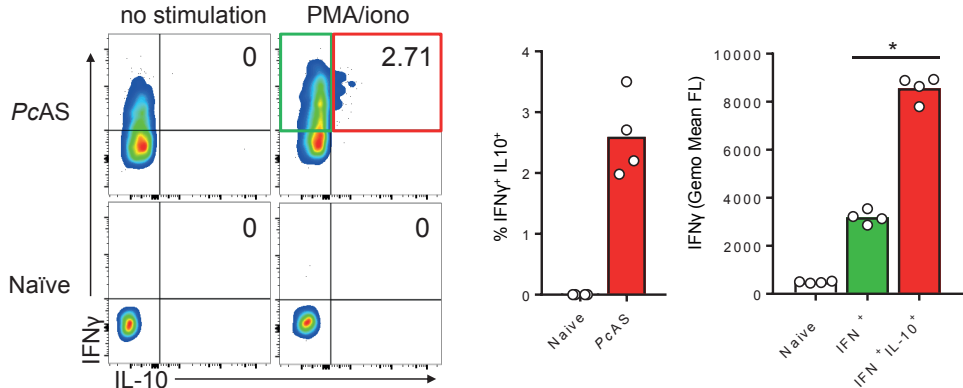


**B**

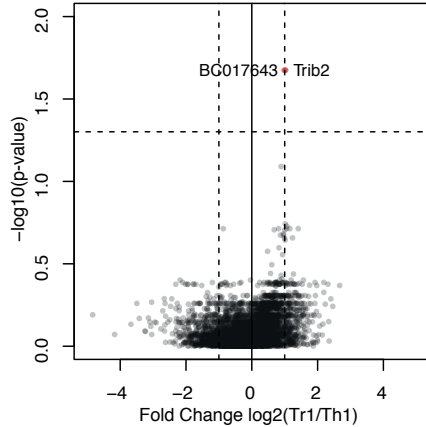


- Uninfected (pre-transfer)
- Uninfected (day 7)
- Day 2
- Day 3
- Day 4
- Day 7
- Experiment 1
- Experiment 2

**C**



**D**



**E**

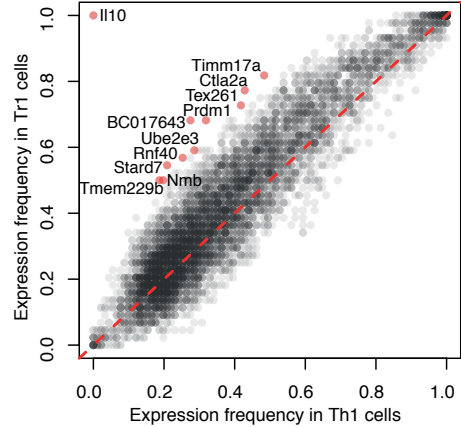


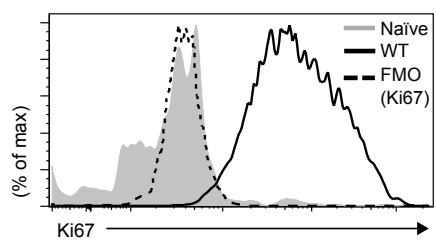
**Fig. S15.** IL-10- and IFN $\gamma$ -co-producing Tr1 cells derive from Th1 cells.

- (A)** The expression kinetics of *Ifng* (left) and *Il10* (right) according to the GPfates model. Curves represent the expression patterns associated with the Th1 (red) and the Tfh (blue) trends.
- (B)** Co-expression of *Ifng* and *Il10* in single cells. The colors of the data points represent time points and the shapes represent cells from two replicate experiments. Tr1 cells were defined as cells expressing both *Ifng* and *Il10* at  $\geq 10$  TPM. Th1 cells were defined as cells expressing *Ifng* but not *Il10* at  $\geq 10$  TPM.
- (C)** Representative FACS plots (gated on CD45.1 $^+$  CD4 $^+$  TCR $\beta$  $^+$  live singlets), proportions and mean fluorescence intensities of IFN $\gamma$  (Th1) and IL-10 $^+$  IFN $\gamma^+$  (Tr1) PbTII cells ( $10^4$  transferred) with or without *ex vivo* PMA/ionomycin restimulation at day 7 post-infection with *PcAS*. Statistics: Mann-Whitney U test; \*p<0.05. Geom Mean FL; Geometric Mean Fluorescence Level.
- (D)** Differential expression genes between day 7 Th1 cells and Tr1 cells, as defined in (B). All genes expressed in at least 20% of the single cells were included in the analysis. P-values were calculated using Wilcoxon Rank Sum test, and adjusted for multiple testing using Benjamini & Hochberg correction. The top hit *Il10* is not shown.
- (E)** Analysis of expression frequency for all genes in the day 7 Th1 cells and Tr1 cells, as defined in (B). Expression frequency was defined as the number of cells where the transcript was detected,

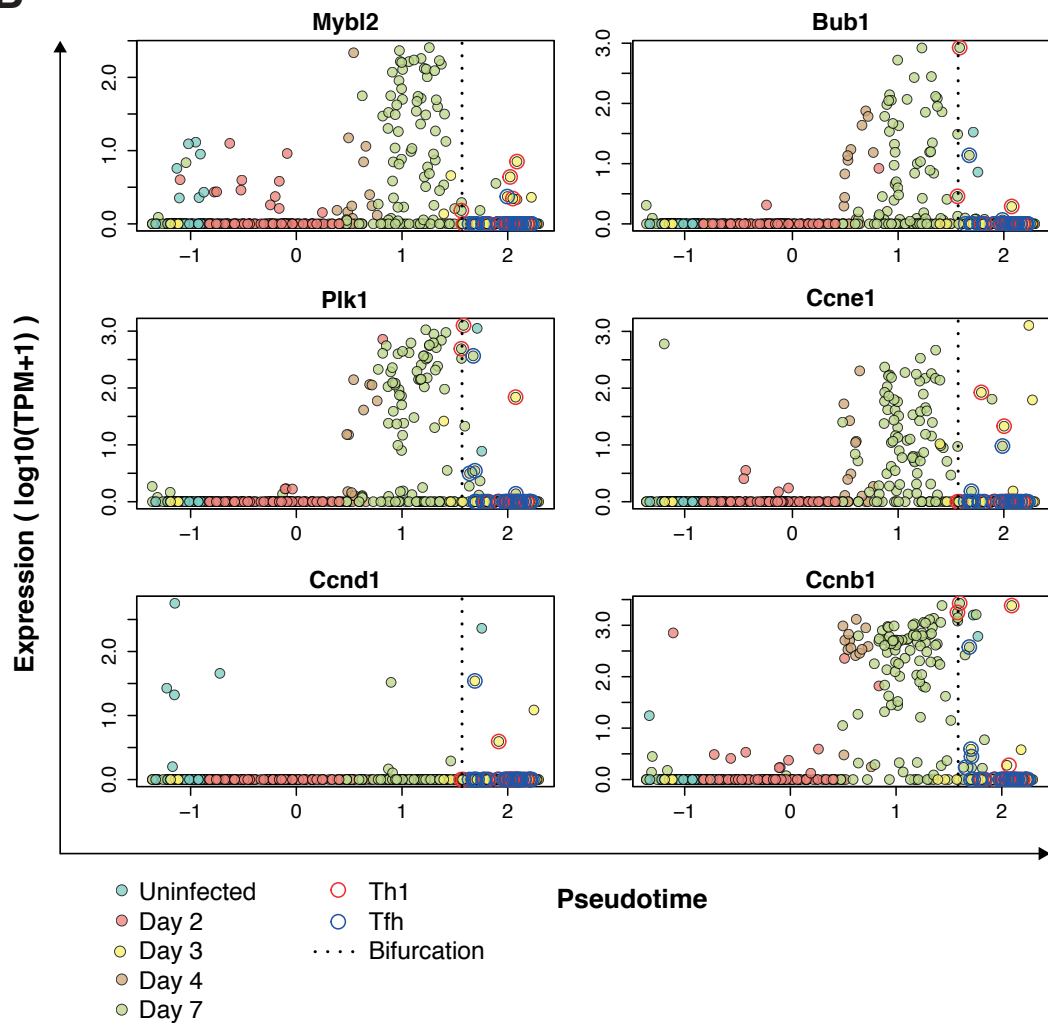
divided by total number of cells. Genes with at least 0.3 difference in expression frequency between Th1 and Tr1 cells are highlighted in red.

**Figure S16**

**A**



**B**



**C**

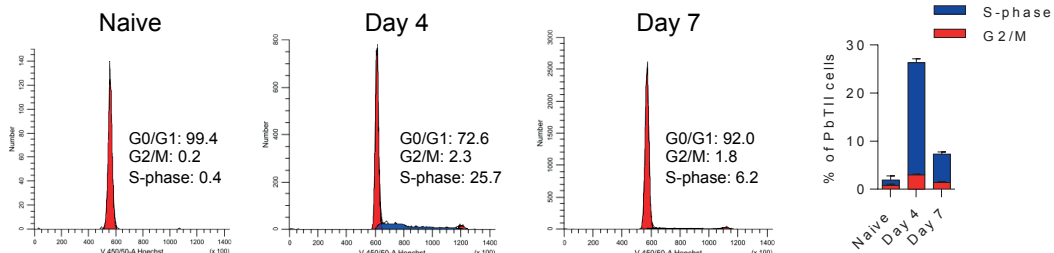


**Fig. S16.** Proliferative burst of activated PbTII cells.

- (A)** Fluorescence minus one (FMO) control for expression of Ki67 by splenic PbTII cells from a day 7-infected mouse.
- (B)** The expression of established proliferation genes (*31*) along pseudotime.
- (C)** ModFit plots and proportions of PbTII cells in G0/G1, G2/M and S-phase of cell cycle as determined by Hoechst staining.

**Figure S17**

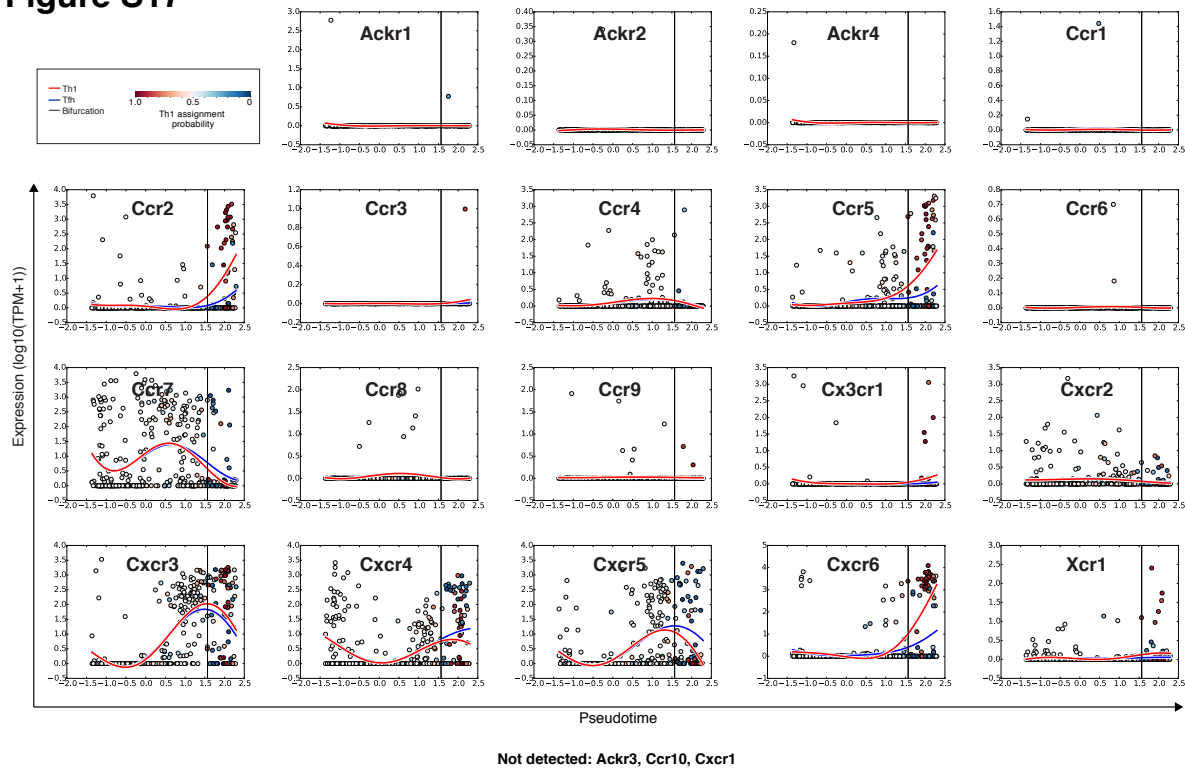
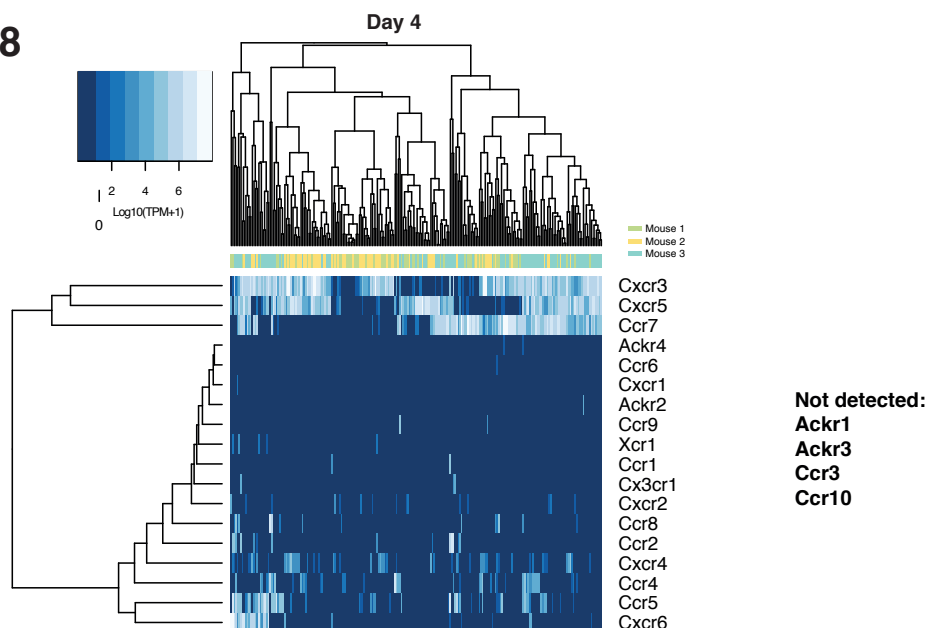
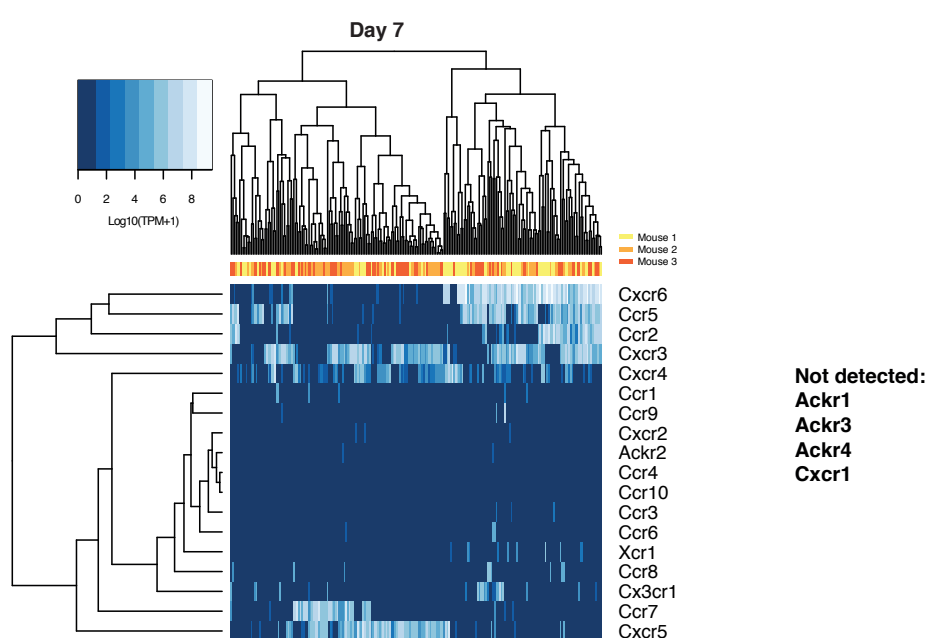


**Fig. S17.** Kinetics of chemokine receptor expression during *PcAS* infection according to the GPfates model. Curves represent the expression patterns associated with the Th1 (red) and the Tfh (blue) trends.

**Figure S18**  
**A**



**B**



**C**

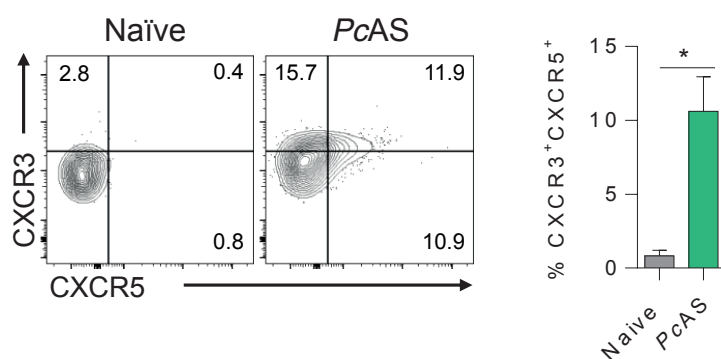


**Fig. S18.** Co-expression of chemokine receptors at single-cell level during *PcAS* infection.

**(A)** The expression of chemokine receptors in single cells at day 4 post infection.

**(B)** The expression of chemokine receptors in single cells at day 7 post infection.

**(C)** Representative FACS plots and proportions of splenic PbTII cells co-expressing CXCR5 and CXCR3 in naive (gray; n=3) or infected mice (green; n=6) at 4 days post-infection with *PcAS*.

Results are representative of two independent experiments. Statistics: Mann-Whitney U test

\*p<0.05.

## Figure S19

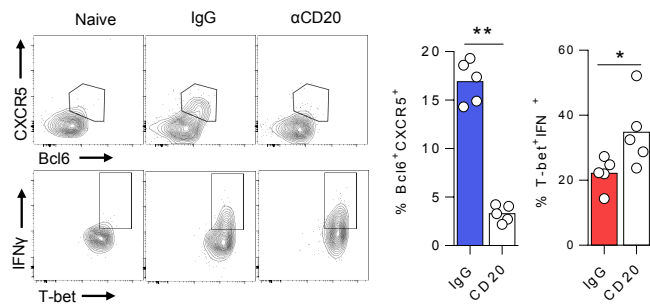


**Fig. S19.** B cells are essential for Tfh responses in PbTII cells during *PcAS* infection.

Representative FACS plots (gated on CD4+ TCRβ+ CD45.1+ live singlets) of splenic PbTII cells, showing proportions exhibiting Tfh (Bcl6+ CXCR5+) and Th1 (Tbet+ IFNγ+) phenotypes in WT mice (receiving 104 PbTII cells), treated with anti-CD20 monoclonal antibodies (0.25mg) to deplete B-cells, or control IgG, and infected for 7 days with *PcAS*. Individual mice data (n=5) shown in summary graph. Mann-Whitney U test \*p<0.05; \*\*p<0.01. Results are representative of two independent experiments.

## Figure S20

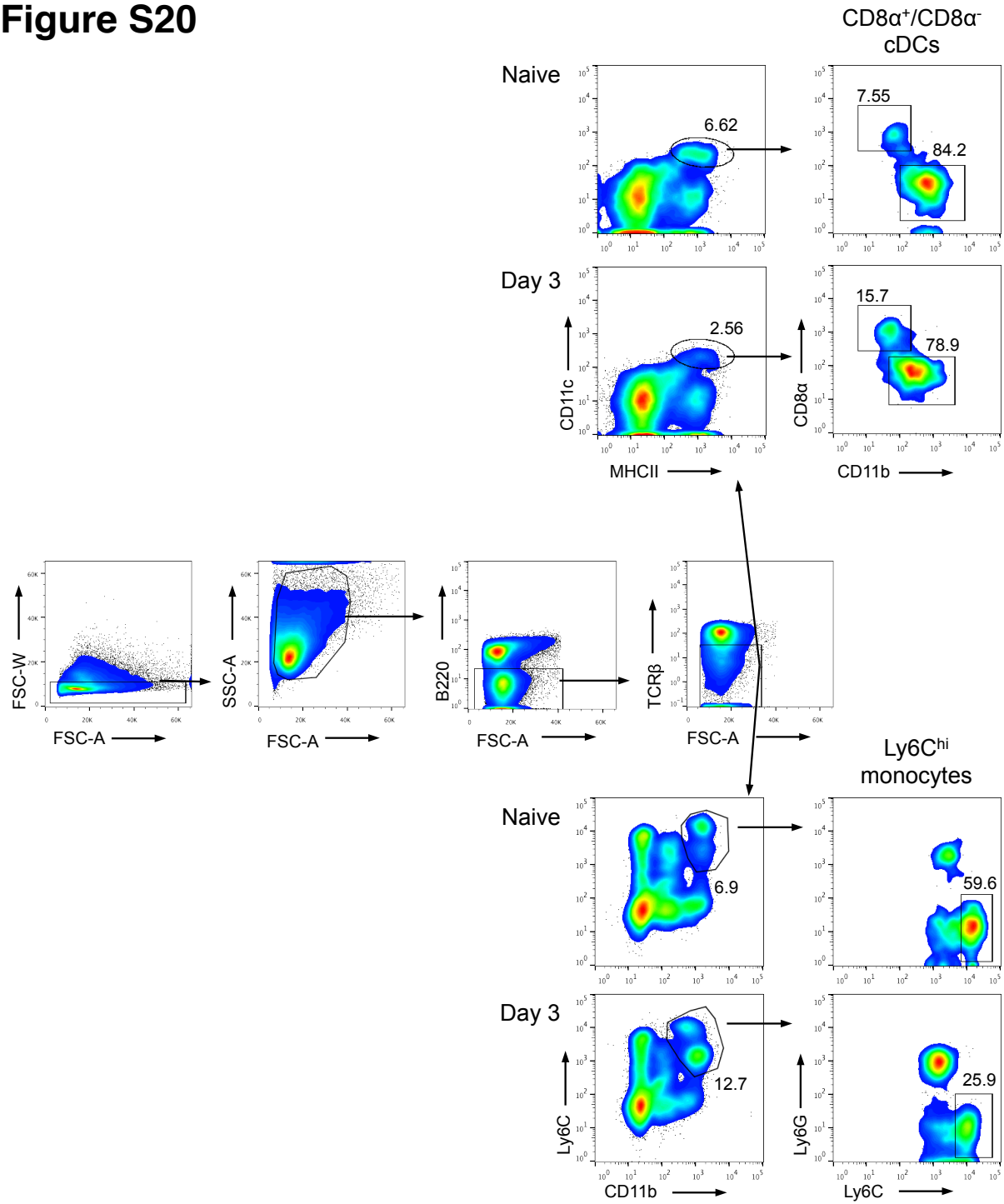


**Fig. S20.** Sorting strategy for myeloid cells.

Representative FACS plots showing sorting strategy for CD8 $\alpha$ <sup>+</sup> and CD11b<sup>+</sup> cDC, and Ly6C<sup>hi</sup> inflammatory monocytes from the spleens of naive and 3-day *PcAS*-infected mice.

## Figure S21

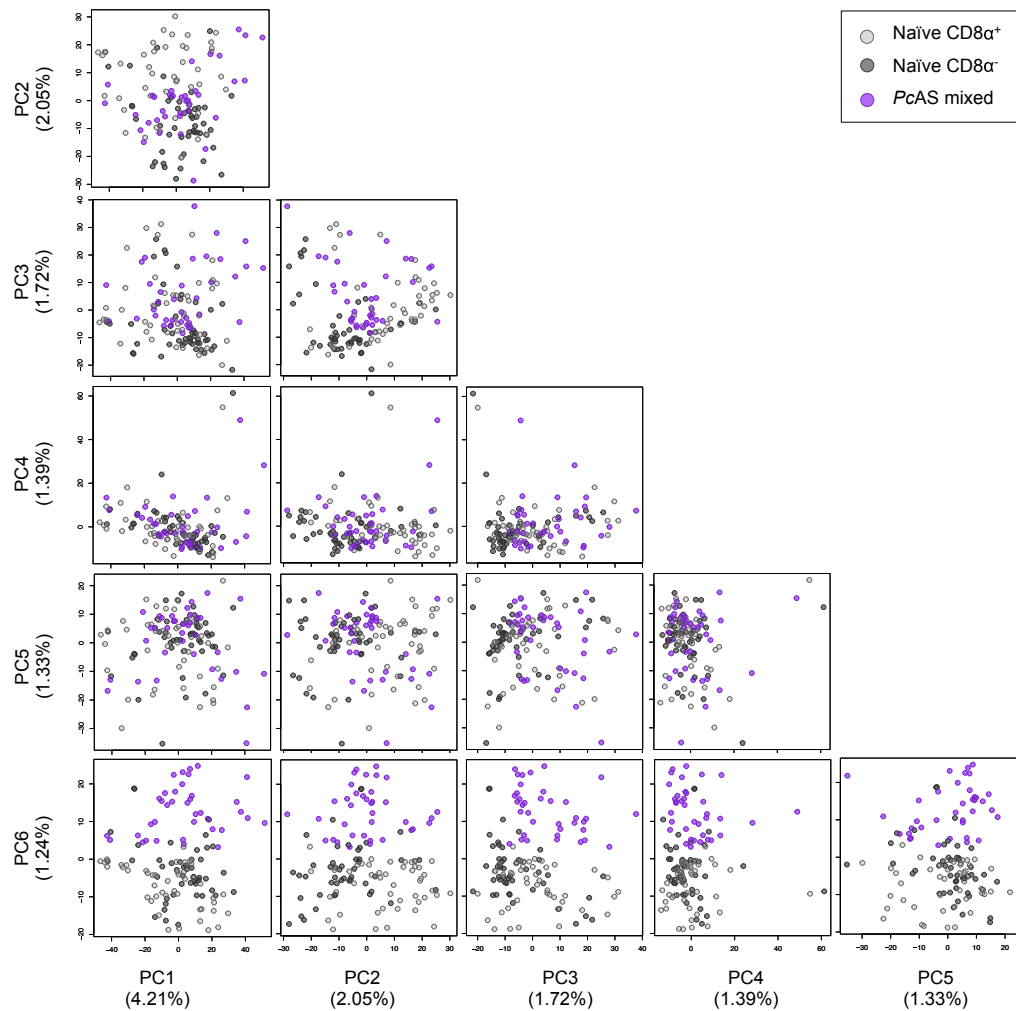


**Fig. S21.** Principal Component Analysis of cDCs from naïve and infected mice.

Results of Principal Component (PC) Analysis on scRNA-seq mRNA reads (filtered by minimum expression of 100 TPM in at least 2 cells) from 131 single splenic naïve CD8 $\alpha^+$  and CD8 $\alpha^-$  and mixed day 3 *PcAS*-infected cDC. PC1-PC6 shown. Axis labels show proportional contribution of respective PC.

## Figure S22

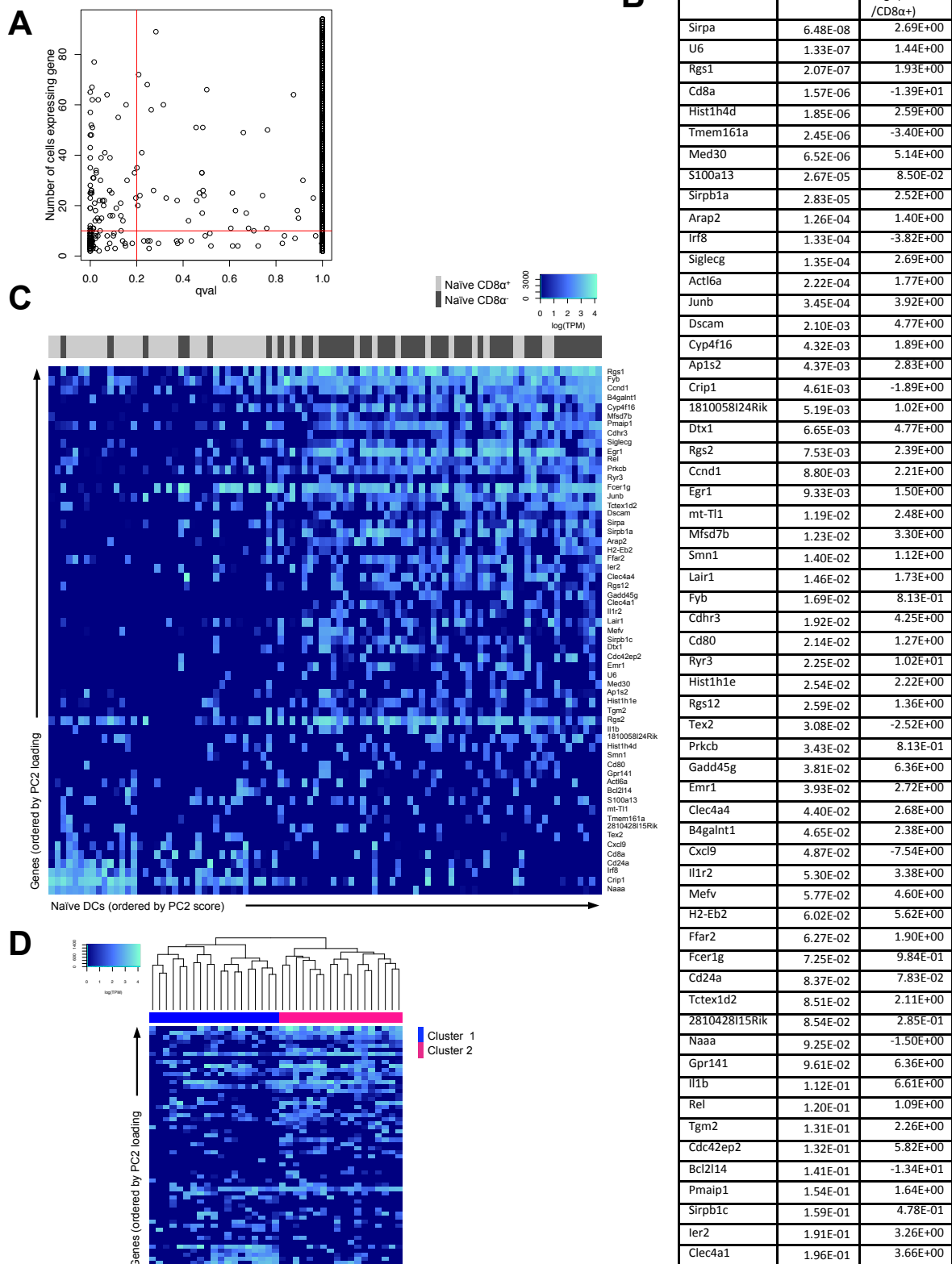


**Fig. S22.** Differential gene expression between single splenic CD8 $\alpha^+$  and CD8 $\alpha^-$  cDCs.

- (A)** Results of differential gene expression analysis between naïve splenic CD8 $\alpha^+$  and CD8 $\alpha^-$  cDCs, for all genes expressed in greater than 2 cells.
- (B)** Complete list of differentially-expressed genes between naïve CD8 $\alpha^+$  and CD8 $\alpha^-$  cDCs, which were expressed in >10 cells of either subset with a qval <0.2 as determined in (A).
- (C)** Heatmap of naïve cDCs ordered by PC2 (Fig. 6A) and expression of genes from (B) ordered by PC2 loading in (Fig 6A).
- (D)** Heatmap examining hierarchical clustering of mixed CD8 $\alpha^+$  and CD8 $\alpha^-$  CD11b $^+$  day 3-infected cDCs (cell-sorted and mixed at a ratio of 50:50 prior to scRNA-seq) using differentially expressed genes from (B) ordered by PC2 loading shown in (Fig 6A).

## Figure S23

Gene	Log2 (Fold change)	qval
Tgtp1	4.36E+00	4.84E-11
Tgtp2	2.78E+00	1.68E-10
Ifi47	3.56E+00	4.23E-10
Kdm6b	4.25E+00	1.22E-09
Actb	1.62E+00	1.01E-07
Igtp	4.00E+00	1.43E-07
AC124762.1	3.06E+00	3.69E-07
Gm15427	-9.78E-01	1.51E-06
Stat1	2.49E+00	1.92E-06
U6	-3.31E+00	8.27E-06
Snora31	9.27E-01	9.92E-06
Nlrc5	2.09E+00	1.43E-05
Gm12250	5.43E+00	1.61E-05
Zbp1	4.87E+00	5.59E-05
Gbp4	3.41E+00	1.82E-04
R3hdm4	2.19E+00	2.52E-04
Slc39a1	3.20E+00	7.09E-04
Gm10800	6.42E-01	8.35E-04
Cxcl10	3.43E+00	1.81E-03
Alkbh5	3.20E+00	1.98E-03
Cxcl9	2.42E+00	2.38E-03
Dtx3l	1.74E+00	4.69E-03
Wtap	2.85E+00	4.87E-03
AC131780.3	1.11E+00	5.07E-03
Gbp3	1.40E+00	5.89E-03
Wac	2.87E+00	8.31E-03
Pml	2.96E+00	1.35E-02
Arf4	1.89E+00	1.56E-02
Irif1	1.44E+00	2.27E-02
Gbp2	2.12E+00	4.55E-02

!

**Fig. S23.** Differentially expressed genes between single naïve and day 3 *PcAS*-infected cDCs. List of differentially expressed genes, expressed in >10 cells ( $\text{qval} < 0.05$ ) between naïve and day 3-infected cDCs. Mean TPM fold-change in gene expression relative to naïve levels.

## Figure S24

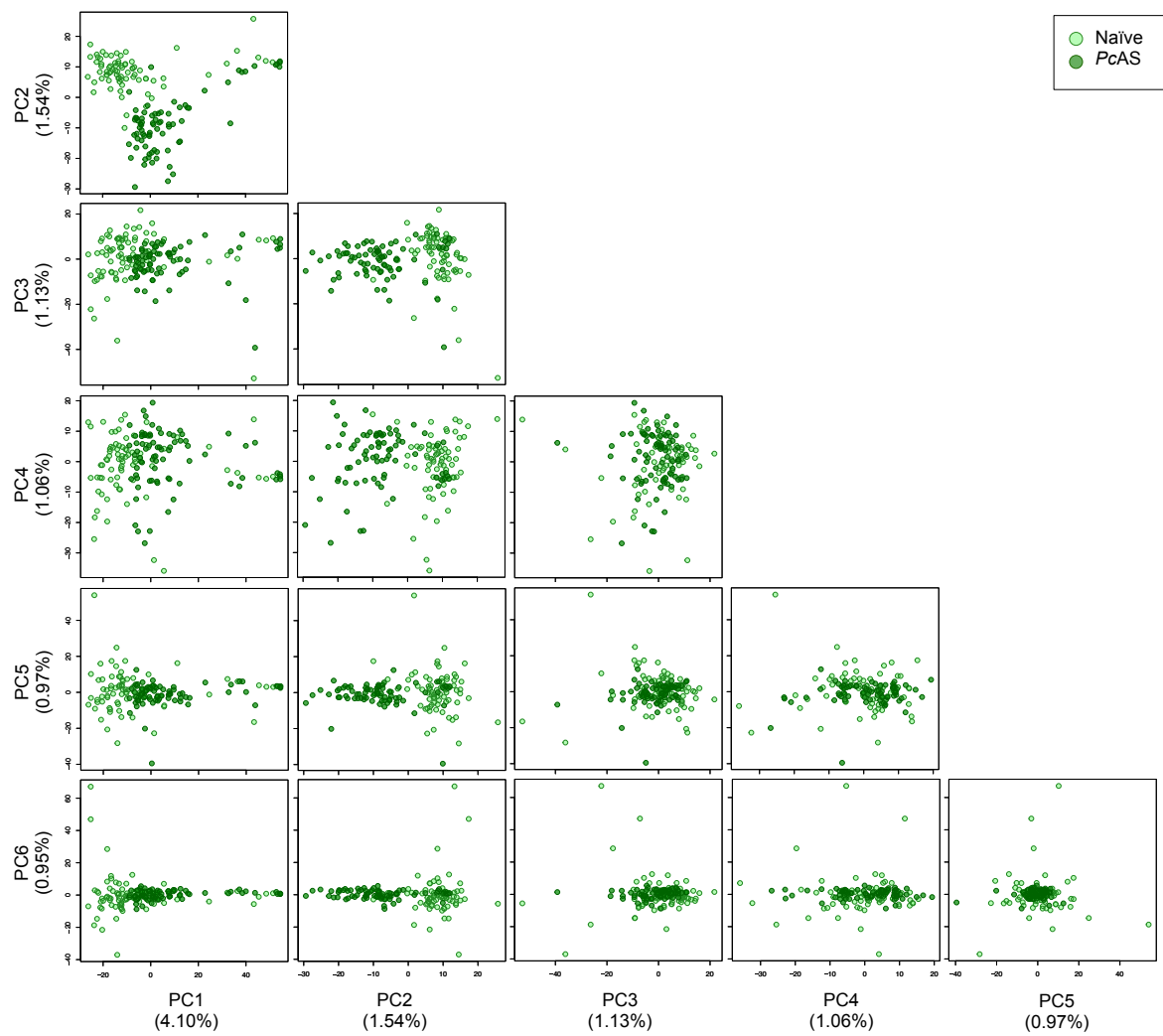


**Fig. S24.** Principal Component Analysis of Ly6C<sup>hi</sup> monocytes from naïve and infected mice.

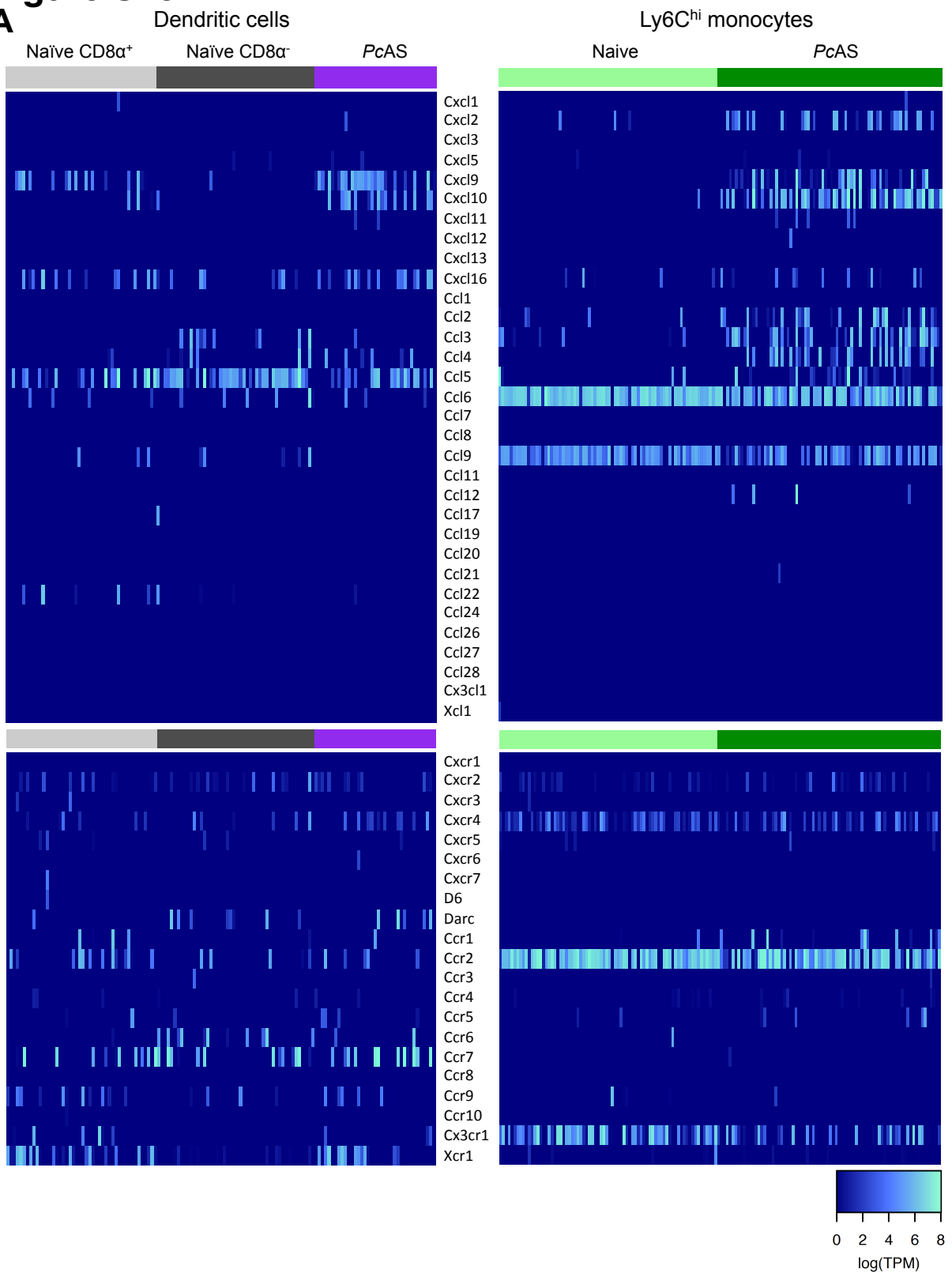
Results of Principal Component (PC) Analysis using scRNA-seq mRNA reads (filtered by minimum expression of 100 TPM in at least 2 cells) of 154 single splenic Ly6C<sup>hi</sup> monocytes from naïve and infected mice. PC1-PC6 shown. Axis labels show proportional contribution of respective PC.

## Figure S25

Gene	Log2 (Fold change)	qval	Gene	Log2 (Fold change)	qval
Gbp2	5.34E+00	2.14E-33	Lilra6	-2.05E+00	4.38E-04
Egr1	5.03E+00	1.11E-25	Atp2b1	-1.49E+00	4.72E-04
Ifi47	3.25E+00	6.85E-20	Ptplad2	-1.12E+00	8.36E-04
Cxcl10	9.85E+00	8.78E-20	Dnm1l	-2.68E+00	8.92E-04
Irf1	3.97E+00	3.93E-17	Stk4	-1.04E+00	1.07E-03
Tgtp1	1.25E+01	9.12E-17	Hmgb2	-2.08E-01	1.16E-03
Tgtp2	3.86E+00	7.32E-15	Mar-01	-1.99E+00	1.32E-03
Stat1	2.75E+00	2.36E-10	Ifit2	3.96E+00	1.44E-03
Gbp4	5.77E+00	1.34E-09	Kif4	-2.63E+00	1.59E-03
Igtp	2.70E+00	1.46E-09	Calm2	-8.75E-01	1.61E-03
Fam26f	4.71E+00	1.56E-08	Ifcg3	-1.45E+00	2.17E-03
Ifi205	2.56E+00	6.71E-08	Dnase1l3	3.16E+00	2.21E-03
Gbp7	2.72E+00	9.43E-07	Nrp2	3.68E+00	2.52E-03
U2	3.96E+00	9.47E-07	Zbp1	1.92E+00	3.89E-03
Gbp6	7.60E+00	1.30E-06	Gbp9	1.57E+00	3.91E-03
Irgm1	2.55E+00	2.23E-06	Tsc22d3	-1.15E+00	3.97E-03
Gbp3	3.65E+00	3.14E-06	Rel1	-2.69E+00	4.03E-03
Serpina3g	1.05E+01	4.62E-06	Srsf2	-1.23E+00	4.08E-03
Nfkbiz	3.22E+00	7.52E-06	Jun	2.22E+00	5.32E-03
Gm17334	3.71E+00	8.59E-06	Hnrnph1	-2.23E+00	5.49E-03
Gbp5	5.77E+00	9.75E-06	Itgb2	-1.02E+00	5.81E-03
D4Wsu53e	-1.29E+00	1.86E-05	Ifit3	2.67E+00	5.90E-03
Ceacam1	-1.49E+00	1.94E-05	Eif4a2	-1.39E+00	6.05E-03
Gpcpd1	-3.58E+00	1.98E-05	Rps6ka1	-1.72E+00	6.59E-03
Hpgd	-2.92E+00	2.11E-05	Rtp4	2.19E+00	6.62E-03
Pim1	2.21E+00	2.51E-05	Sfr1	-7.00E-01	6.70E-03
Cd244	-2.01E+00	3.26E-05	Fam107b	-1.63E+00	7.79E-03
Cd40	1.70E+00	7.05E-05	Tmem164	-1.11E+00	7.98E-03
Cd274	5.40E+00	8.55E-05	Mnda	1.14E+00	9.66E-03
Cd300lb	-1.80E+00	1.03E-04	Glg1	-7.70E-01	1.06E-02
Kdm6b	2.71E+00	1.30E-04	Irgm2	3.51E+00	1.10E-02
CT572998.1	4.26E+00	1.39E-04	Emilin2	-1.78E+00	1.16E-02
Nfkbia	2.51E+00	1.47E-04	TIK1	-2.16E+00	1.19E-02
Cxcl2	5.03E+00	1.88E-04	Tmem126b	-6.42E+00	1.47E-02
Ccl3	5.80E+00	2.16E-04	Lrp1	-1.51E+00	1.68E-02
Pira2	-2.11E+00	2.24E-04	Zzef1	-4.02E+00	1.78E-02
Susd3	-1.73E+00	2.88E-04	Pik3cg	-1.62E+00	1.89E-02
Nfic	-4.22E+00	3.26E-04	Camk1d	-3.82E-01	1.97E-02
Ogt	-1.84E+00	3.37E-04	Cd84	-1.75E+00	1.98E-02
Mll3	-2.64E+00	3.72E-04	Vps13c	-1.66E+00	2.08E-02
Mast3	-9.02E+00	3.78E-04	Cd300ld	-4.31E+00	2.15E-02
Ptpre	-1.63E+00	4.04E-04	Atf3	2.59E+00	2.17E-02
Ccr12	4.81E+00	4.17E-04	Emr4	-1.48E+00	2.27E-02
			Cx3cr1	-2.06E+00	2.34E-02
			Nedd8	-4.54E-01	2.45E-02

**Fig. S25.** Differentially expressed genes between single Ly6C<sup>hi</sup> monocytes from naïve and day 3 *PcAS*-infected mice.

List of differentially expressed genes, expressed in >10 cells ( $\text{qval} < 0.05$ ) between Ly6C<sup>hi</sup> monocytes from naïve and day 3-infected mice. Mean TPM fold-change in gene expression relative to naïve levels.

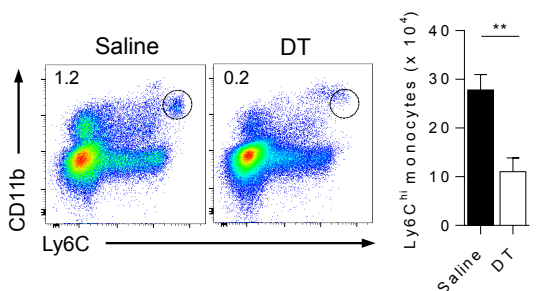
**Figure S26****A**

**Fig. S26.** Expression of immune signalling genes by cDCs and monocytes.

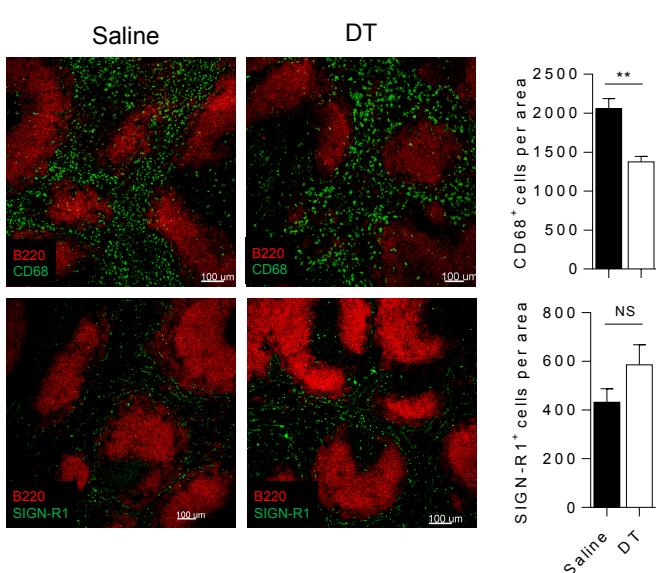
**(A-C)** Heatmaps showing normalised mRNA expression of select **(A)** chemokines, **(B)** costimulatory molecules and **(C)** cytokines and respective receptors (rows) by single splenic cDCs and Ly6C<sup>hi</sup> monocytes (columns) from naïve or 3-day *PcAS*-infected mice.

## Figure S27

**A**



**B**



**C**

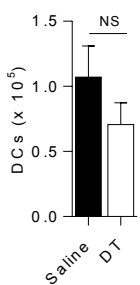


**Fig. S27.** Myeloid cell depletion in *LysM*<sup>Cre</sup> x *iDTR* mice.

*LysM*<sup>Cre</sup> x *iDTR* mice were infected with *PcAS*, and treated 3 days later with DT (10ng/g intraperitoneal injection) or control saline (n=6 per group). 24 hours later spleens were harvested for cellular compositional analysis:

**(A)** Representative FACS plots enumerating splenic inflammatory monocytes ( $\text{Ly6C}^{\text{hi}}$   $\text{CD11b}^{\text{hi}}$   $\text{Ly6G}^- \text{B220}^- \text{TCR}\beta^-$ ).

**(B)** Representative fluorescence micrographs showing spleen tissue sections co-stained for B cells (B220 in red) and macrophages (CD68 (top panel) or SIGN-R1 (bottom panel) in green) and summary graphs of average cell number in three fields of view covering the total cross section of a spleen.

**(C)** Flow cytometric enumeration of splenic cDC ( $\text{CD11c}^{\text{hi}}$   $\text{MHCII}^{\text{hi}}$   $\text{B220}^- \text{TCR}\beta^-$ ).